HHS Public Access

Author manuscript

Cell Rep. Author manuscript; available in PMC 2024 July 02.

Published in final edited form as:

Cell Rep. 2024 June 25; 43(6): 114294. doi:10.1016/j.celrep.2024.114294.

TBK1 is ubiquitinated by TRIM5α to assemble mitophagy machinery

Bhaskar Saha[1,2], **Hallvard Olsvik**[3], **Geneva L Williams**[4], **Seeun Oh**[1], **Gry Evjen**[3], **Eva Sjøttem**[3], **Michael A Mandell**[1,5,*]

[1]Department of Molecular Genetics and Microbiology, University of New Mexico Health Sciences Center, Albuquerque, NM 87131 USA

[2]Present address: Department of Cell and Molecular Biology, Manipal School of Life Sciences, Manipal Academy of Higher Education, Manipal, Karnataka, 576104, India

[3]Autophagy Research Group, Department of Medical Biology, University of Tromsø-The Arctic University of Norway, Tromsø, Norway

[4]Biomedical Sciences Graduate Program, University of New Mexico Health Sciences Center, Albuquerque, NM 87131 USA

[5]Autophagy, Inflammation and Metabolism Center of Biomedical Research Excellence, University of New Mexico Health Sciences Center

SUMMARY

Ubiquitination of mitochondrial proteins provides a basis for the downstream recruitment of mitophagy machinery, yet whether ubiquitination of the machinery itself contributes to mitophagy is unknown. Here, we show that K63-linked polyubiquitination of the key mitophagy regulator TBK1 is essential for its mitophagy functions. This modification is catalyzed by the ubiquitin ligase TRIM5α, and is required for TBK1 to interact with and activate a set of ubiquitin-binding autophagy adaptors including NDP52, p62/SQSTM1, and NBR1. Autophagy adaptors, along with TRIM27, enable TRIM5α to engage with TBK1 following mitochondrial damage. TRIM5α's ubiquitin ligase activity is required for the accumulation of active TBK1 on damaged mitochondria in Parkin-dependent and Parkin-independent mitophagy pathways. Our data support a model in which TRIM5α provides a mitochondria-localized, ubiquitin-based, self-amplifying assembly platform for TBK1 and mitophagy adaptors that is ultimately necessary for the recruitment of the core autophagy machinery.

INTRODUCTION

Removal of unwanted or dysfunctional mitochondria is essential for cellular health. This is accomplished through mitophagy, an autophagy-based system for the selective degradation of mitochondria in lysosomes. Mitophagy is activated in response to mitochondrial

*Lead contact: mmandell@salud.unm.edu.

Author contributions

B.S., G.L.W., S.O., G.E., H.O., and M.A.M performed research; B.S., H.O., E.S., and M.A.M designed research and analyzed data; B.S. and M.A.M. wrote the paper. The authors declare that they have no conflict of interest.

damage or for the elimination of mitochondria as part of cellular development (e.g. reticulocyte maturation)[1,2]. Alterations in mitophagy have been linked with cardiovascular, metabolic, or neurodegenerative diseases and cancer[3–5]. As such, there has been intensive interest in uncovering the molecular mechanisms underlying how cells selectively identify mitochondria for mitophagy-based elimination[6].

Several non-redundant mitophagy pathways have evolved. The molecular details of how mitochondria are identified by these pathways differ; nevertheless, they all involve the sequential and self-amplifying localization of a conserved set of autophagy proteins to mitochondria[7,8]. Elegant studies have shown that the recruitment of the ULK1/FIP200 complex to mitochondria is necessary and sufficient for mitophagy induction[7–10]. This complex can stimulate the mitochondrial localization and activation of downstream factors required for the initiation and execution of autophagosome formation. The optimal recruitment of the ULK1/FIP200 complex to damaged mitochondria is dependent on the accumulation or presentation of proteins on the mitochondria's cytoplasmic face that mark it for recognition by the autophagy machinery[11–15]. Ubiquitination of proteins on the outer mitochondrial membrane is one such marker[16,17]. This ubiquitin can serve as a ligand for ubiquitin-binding autophagy adaptor proteins. These adaptors interact with the ULK1/FIP200 complex and other autophagy proteins (e.g. LC3s and GABARAPs) and can enable their recruitment to ubiquitinated mitochondria[8,9,14,18,19].

Mitophagy can prevent aberrant immune activation in cell lines and in model organisms[20–22], providing a possible explanation for how it maintains organismal health. The inability to clear damaged mitochondria by mitophagy can result in the cytosolic accumulation of immune-stimulatory mitochondrial molecules, leading to the activation of antiviral signal transduction pathways[23]. These pathways converge on TANK-binding kinase 1 (TBK1), which can induce the expression of hundreds of genes with antiviral functions by phosphorylating and activating IRF-family transcription factors[24]. Remarkably, TBK1 is also an essential player in mitophagy[14,17], suggesting a linkage between mitochondrial quality control and antiviral defense systems. TBK1 is among the first proteins recruited to mitochondria following damage[14,25,26]. TBK1 binds to and phosphorylates autophagy adaptors, increasing their affinity for both ubiquitin and for ULK1/FIP200 complex components[8,27,28]. TBK1 can also initiate mitophagy by directly activating the class III phosphatidylinositol 3-kinase complex[29]. Through these actions, TBK1 orchestrates the recruitment of the rest of the autophagy machinery to mitochondria. To act in mitophagy, TBK1 must be activated. Since the activation of TBK1 is mediated by trans-autophosphorylation[30], the clustering of multiple TBK1 dimers at the mitochondria is a likely prerequisite for mitophagy, yet the mechanistic basis for how TBK1 is activated on damaged mitochondria has not been fully elucidated.

We recently showed that another antiviral protein, TRIM5α, also plays key roles in multiple distinct mitophagy pathways[31]. TRIM5α is a member of the tripartite motif (TRIM) protein family. The TRIM family consists of more than 80 genes in humans, most of which encode a RING ubiquitin ligase domain at their N-terminus[32]. Nearly two decades ago, TRIM5α from rhesus macaques was shown to restrict HIV-1 infection[33]. This finding, and many more that came afterwards, established TRIMs as having roles in antiviral defense and innate

immunity[34–37]. Interestingly, multiple GWAS studies have found associations between TRIM5α and metabolic or cardiovascular diseases[38–41], suggesting that TRIM5α also plays homeostatic roles. Accordingly, we showed that TRIM5α mediated the recruitment the ULK1/FIP200 complex to mitochondria under mitophagy-inducing conditions and blunted mitochondrial damage-induced immune activation[31]. However, the mechanism underlying TRIM5α-dependent mitophagy is unknown.

Here, we show that TRIM5α and TBK1 cooperate to execute the elimination of damaged mitochondria through autophagy. We show that mitochondrial damage induces TRIM5α-mediated, K63-linked, poly-ubiquitination of TBK1 and itself. This results in the formation of a multi-protein scaffold including TRIM5α, TBK1, and mitophagy adaptors that enables TBK1 activation and the subsequent assembly of mitophagy machinery on damaged mitochondria. Collectively, these findings establish an unexpected functional convergence of two key antiviral proteins in mitochondrial quality control, demonstrate that ubiquitination-dependent activation of TBK1 is an essential regulatory step in mitophagy initiation, and position TRIMs at a central hub in orchestrating mitophagy.

RESULTS

TRIM5α recruits active TBK1 to damaged mitochondria.

We reported that TRIM5α is required for two distinct ubiquitin-dependent mitophagy pathways: Parkin-dependent mitophagy induced by CCCP and for Parkin-independent mitophagy induced by ivermectin[31]. Proteomic analysis indicated a possible interaction between TRIM5α and TBK1[31]. Since TBK1 is a required factor for both CCCP- and ivermectin-induced mitophagy pathways[14,17], we hypothesized that TRIM5α might engage TBK1 in mitophagy. To test this concept, we first confirmed the involvement of both TRIM5 and TBK1 in mitophagy using the well-established mitoKeima assay for delivery of mitochondria to acidified organelles[9]. As expected, Huh7 cells lacking TBK1 showed markedly reduced mitophagy in this assay (Figure S1A). Mitophagy was also significantly reduced in TRIM5 knock-out Huh7 cells, albeit to a lesser extent that what was seen with the TBK1 knockout cells (Figure S1A). We next determined whether mitochondrial damaging agents could increase TRIM5α-TBK1 interactions. Under basal conditions, GFP-tagged TRIM5α immunoprecipitated myc-TBK1 (Figure 1A, B). Mitophagy inducers CCCP (Figure 1A) or ivermectin (Figure 1B) both reproducibly increased the abundance of TBK1 in protein complexes with GFP-TRIM5α. When active, TBK1 is phosphorylated at serine 172 (pTBK1). We found that pTBK1 co-immunoprecipitated with TRIM5α, indicating that TRIM5α interacts with active TBK1 (Figure 1A, B). Both CCCP and ivermectin treatments increased the ability of endogenous TBK1 to co-immunoprecipitate endogenous TRIM5α from Huh7 cell lysates (Figure S1B). Time course experiments showed that interactions between GFP-TRIM5α and myc-TBK1 increased within the first 30 minutes following mitochondrial uncoupling with CCCP (Figure S1C). Coincidently with the increased TRIM5α-TBK1 interaction, we also observed the appearance of high molecular weight (>250 kDa) bands detected with anti-GFP antibody, indicative of post-translational modifications of TRIM5α in response to mitochondrial damage. Stably expressed HA-tagged TRIM5α colocalized with endogenous pTBK1 in HeLa cells. This colocalization

was more prevalent in cells following mitochondrial uncoupling with CCCP and was found to be closely associated with mCherry-Parkin signal on damaged mitochondria (Figure 1C). Ivermectin treatment also increased colocalization between HA-tagged TRIM5α and endogenous pTBK1 in ivermectin-treated HeLa cells (Figure S1D). Proximity ligation (PLA) can be used to identify protein-protein interactions within 40 nm *in situ*, with positive PLA signal being detected as a fluorescent punctum. We observed numerous PLA signals indicating TRIM5α-TBK1 interactions in both untreated and CCCP-treated HeLa cells (Figure 1D). Most of these PLA signals were found to colocalize with Parkin-decorated mitochondria following CCCP treatment, indicating that TRIM5α-TBK1 complexes form on the surface of damaged mitochondria.

We next tested whether TRIM5α was important for recruiting or retaining active pTBK1 to mitochondria following mitochondrial damage. In WT Huh7 cells transfected with myc-TBK1, either CCCP or ivermectin treatment increases the abundance of pTBK1 in mitochondrial fractions (Figure 1E and Figure S1E). In contrast, pTBK1 was not enriched in mitochondrial fractions from cells lacking the TRIM5 gene (Figure 1E and Figure S1E). Transient expression of GFP-TRIM5α in TRIM5 knockout cells restored the CCCP-induced pTBK1 accumulation on damaged mitochondria (Figure 1F). Consistent with these results, pTBK1 showed reduced colocalization with the mitochondrial marker TIM23 in TRIM5 knockout Huh7 cells relative to control Huh7 cells under CCCP-treatment conditions (Figure S1F). Together, these data show a requirement for TRIM5α in localizing active TBK1 to mitochondria following the induction of Parkin-dependent and Parkin-independent mitophagy.

TBK1 is required for TRIM5α-mediated recruitment of autophagy proteins to damaged mitochondria.

The protein Sequestosome-1 (SQSTM1, also p62) is recruited to ubiquitinated mitochondria[42] and is phosphorylated at serine 349 (pSQSTM1) by TBK1[27]. By high content imaging, we observed a robust increase in the number of pSQSTM1 puncta following either CCCP or ivermectin treatment in wild type Huh7 cells that was substantially abrogated in TRIM5 knockout cells (Figure 2A, B). This demonstrates that TRIM5α controls the ability of TBK1 to phosphorylate mitophagy-relevant substrates, suggesting that TBK1 acts downstream of TRIM5α in mitophagy. We previously showed that the recruitment of several autophagy proteins, including members of the ULK1/FIP200 complex, to damaged mitochondria is dependent on TRIM5α[31]. Using mitochondrial fractionation experiments (Figure S2A), we found that ectopic expression of TRIM5α in TRIM5 knockout cells rescues this phenotype (Figure S2B). We generated TRIM5-TBK1 double knockout cells (Figure S2C) to test whether TBK1 is required for TRIM5α's ability to recruit autophagy machinery to damaged mitochondria. As expected, expression of GFP-TRIM5α in TRIM5-knockout Huh7 cells increased the CCCP-driven recruitment of total and autophagy-active ULK1 (phosphorylated at Ser555) and of FIP200 to mitochondria (Figure 2C–E). TRIM5α re-expression also enhanced the abundance of TBK1-phosphorylated autophagy adaptors SQSTM1 (phospho-Ser349) and optineurin (phospho-Ser177) in mitochondrial fractions from CCCP-treated cells (Figure 2C, F–G). However, the absence of TBK1 completely abrogated the TRIM5α-dependent localization

of pULK1, FIP200, pSQSTM1, and pOptineurin to mitochondria in response to CCCP. Similarly, treatment with the TBK1 inhibitor BX-795 also prevents the TRIM5α-dependent localization of mitophagy proteins to CCCP-damaged mitochondria (Figure 2H–L). These results establish TBK1 as an essential factor downstream of TRIM5α in mitophagy.

In addition to their actions in mitophagy, both TRIM5α and TBK1 have well-known roles in antiviral defense. TRIM5α can activate the kinase TAK1 to promote the establishment of an NF-κB-dependent antiviral state[43,44], and TBK1 can activate IRF3/7 transcription factors leading to type I interferon expression[45]. We asked how the TRIM5α-TBK1 axis connects with the antiviral activities of these proteins. We used the TAK1 inhibitor (5Z)-7-Oxozeaenol to test whether TAK1 contributed to CCCP-induced mitophagy as measured by the degradation of the mitochondrial inner membrane protein COXII, but saw no effect (Figure S2D, E). We then asked whether TRIM5α could activate antiviral signaling downstream of TBK1. Ectopic expression of TRIM5α in HEK293T cells was sufficient to enhance the abundance of pTBK1 in cells under both basal conditions and following CCCP treatment, possibly through stabilization of total TBK1 (Figure S2F–H). TRIM5α expression also increased the abundance of pSQSTM1 (Figure S2F, I), an autophagy-relevant TBK1 substrate, but only following CCCP treatment. We then used a dual-luciferase reporter system to measure the effect of TRIM5α expression on TBK1-dependent activation of interferon signaling. As previously reported[43], TRIM5α expression induces activation of NF-κB driven luciferase (Figure S2J). However, TRIM5α expression actually reduced the ability of TBK1 to promote activation of an interferon-stimulated response element (Figure S2K). These data indicate that the TRIM5α-activated pool of TBK1 does not promote innate immune signaling and is likely specific to autophagy.

TBK1 ubiquitination by TRIM5α is important for mitophagy.

Previous reports have shown that K63-linked ubiquitination of TBK1 is important for its activity in interferon signaling[46,47]. We hypothesized that TRIM5α's ubiquitin ligase activity, which we previously showed to be important for mitophagy[31], could promote mitophagy through TBK1 ubiquitination. Expression of GFP-TRIM5α in HEK293T cells robustly increased the appearance of high molecular weight TBK1 and the ability of TBK1 to coimmunoprecipitate ubiquitin relative to cells expressing GFP alone (Figure 3A), indicative of TBK1 ubiquitination. This result was also seen when the immunoprecipitation was performed following protein denaturation (Figure S3A), demonstrating that TRIM5α promotes the ubiquitination of TBK1 itself and not a TBK1-interacting protein. We next tested whether TBK1 is ubiquitinated under mitophagy inducing conditions and, if so, how TRIM5α contributes to this. We found that the ubiquitination level of endogenous TBK1 was strongly increased 4 hours after CCCP treatment in wild type HEK293T cells (Figure 3B). While CCCP also increased the level of TBK1 ubiquitination in TRIM5 knockout cells, the effect was much less pronounced than in wild type cells. Time course experiments using epitope-tagged TBK1 and ubiquitin revealed that both CCCP and ivermectin triggered TBK1 ubiquitination as early as 1 hour after treatment in wild type cells that continued to increase up to at least 4 hours after treatment. In these experiments, mitochondrial damage-induced TBK1 ubiquitination was almost entirely dependent on TRIM5α (Figure S3B, C). In experiments using an ubiquitin mutant that was disabled for forming all linkages

except for K63, we found that TRIM5α promotes activating (K63-linked) ubiquitination of TBK1 in response to mitochondrial damage (Figure 3C). Since TBK1 ubiquitination has not previously been described in response to conditions that induce mitophagy or other types of autophagy, we tested whether other known inducers of autophagy, namely amino acid starvation, chemical inhibition of mTOR with pp242, or endomembrane damage caused by LLOMe, could also trigger this posttranslational modification of TBK1 similarly to mitochondrial damage with CCCP. However, of these, CCCP was the only treatment that induced TBK1 ubiquitination (Figure S3D).

We found that TRIM5α's enzymatic activity as an E3 ligase is important for its ability to recruit mitophagy proteins to mitochondria in response to damage. Replacing glutamine 11 in TRIM5α with arginine (E11R) disrupts the ability of TRIM5α to interact with E2 conjugating enzymes and interferes with TRIM5α's enzymatic activity without disrupting its overall structure[43]. Unlike what we see with wild type TRIM5α, expression of TRIM5α E11R does not increase TBK1 ubiquitination (Figure 3D), demonstrating that TRIM5α directly catalyzes TBK1 ubiquitination. TRIM5α E11R was also significantly attenuated in its ability to restore the recruitment of active pTBK1 (Figure 3E, F) and both ULK1 and FIP200 (Figure 3G–I) into mitochondrial fractions following CCCP treatment of TRIM5 knockout cells. Nevertheless, neither E11R nor another E2-binding patch mutant of TRIM5α (L19R) were different from WT in their ability to stabilize TBK1 in whole cell lysates (Figure S3E–G). Together, these results suggest that TRIM5α-mediated TBK1 ubiquitination is a prerequisite step for the mitochondrial localization of active TBK1 in response to mitochondrial damage, but is not required for the overall stabilization of TBK1.

As an alternative approach to assess the importance of TRIM5α-mediated TBK1 ubiquitination, we tested whether the enzymatic removal of ubiquitin from TBK1 (or other TRIM5α-interacting proteins) interfered with mitophagy. This was accomplished using a TRIM5α fusion protein that links the catalytic domain of the UL36 deubiquitinase from herpes simplex virus to TRIM5α's N terminus (Dub-TRIM5α)[48]. As a negative control for these experiments, we also employed a deubiquitinase-dead TRIM5α fusion (Dub*-TRIM5α). While Dub-TRIM5α still somewhat increased TBK1 ubiquitination relative to cells transfected with a control protein (mCherry), it did so to a much lesser extent than did Dub*-TRIM5α (Figure 3J). Dub-TRIM5α failed to restore CCCP-induced mitophagy in TRIM5-knockout Huh7 cells as measured by the degradation of mitophagy proteins (Figure 3K) or the delivery of the mito-mKeima reporter to lysosomes (Figure S3H). In contrast, Dub*-TRIM5α, which is a surrogate for wild type TRIM5α because it has intact ubiquitination function, potently restored mitophagy in these experiments (Figure 3K and Figure S3H). In summary, our data reveal that TRIM5α mediates ubiquitination of TBK1, particularly under conditions of mitochondrial damage. Abrogation of TRIM5α-dependent ubiquitination of TBK1 (or other substrates) impairs TRIM5α's ability to mediate the recruitment of autophagy proteins to damaged mitochondria and to execute mitophagy.

TRIM5α-mediated ubiquitination of TBK1 enhances TBK1 interactions with autophagy adaptors.

Structural and functional studies of TBK1 have demonstrated the importance of TBK1 ubiquitination at lysine residues 30 and 401 for full TBK1 activity in cells[46,47]. We mutated both of these sites in TBK1, replacing them with arginine (TBK1 2X K→R), to test whether these are the predominant ubiquitination sites of TBK1 following mitochondrial damage. As shown in Figure 4A, WT TBK1 showed a basal level of K63-linked poly-ubiquitination that strongly and progressively increased after CCCP treatment. However, the 2X K→R mutant of TBK1 displayed markedly reduced K63-linked ubiquitination in untreated cells and no CCCP-dependent increase in ubiquitination at early time points. At later time points, the 2X K→R TBK1 showed comparable ubiquitination to WT, indicating that additional sites on TBK1 are eventually ubiquitinated under conditions of mitochondrial damage. We next tested whether TRIM5α ubiquitinates TBK1 at K30 and K401 (Figure 4B). Whereas co-expression of GFP-TRIM5α with wild type myc-TBK1 massively increased K63-linked TBK1 ubiquitination, ubiquitination of the 2X K→R mutant of TBK1 was reduced by ~75%. However, TRIM5α clearly promotes ubiquitination of TBK1 at additional sites, since we still observed considerable TRIM5α-dependent ubiquitination of 2X K→R TBK1.

Our data demonstrate that K30 and K401 are the major sites of TRIM5α-dependent TBK1 ubiquitination, and that these sites are ubiquitinated in response to mitochondrial damage. This suggests a model in which K63-linked poly-ubiquitination of TBK1 at K30 and K401 may be important for mitophagy. To test this idea, we assessed mitophagy in TBK1-knockout Huh7 cells transfected with either WT or 2X K→R TBK1 or an irrelevant protein as a negative control using the mito-mKeima assay following ivermectin treatment (Figure 4C and Figure S4A) or by measuring the degradation of mitochondrial proteins following CCCP treatment (Figure S4B, C). In both assays, minimal mitophagy was induced in TBK1 knockout cells expressing an irrelevant protein, in line with the essentiality of TBK1 to both ivermectin- and CCCP-induced mitophagy. Expression of WT TBK1 in these cells substantially boosted the cells' ability to carry out mitophagy. However, expression of the 2X K→R TBK1 mutant was significantly less efficient at promoting mitophagy despite roughly comparable levels of TBK1 protein expression. These data demonstrate that ubiquitination of TBK1 at K30 and K401 is important for TBK1's mitophagy functions.

We next tested whether TBK1 ubiquitination is important for the localization of active pTBK1 to mitochondria following damage. For these experiments, we isolated mitochondrial fractions from TBK1 knockout Huh7 cells that had been reconstituted with either WT or 2X K→R mutant TBK1. While both CCCP and IVM promoted the accumulation of pTBK1 in mitochondrial fractions within 30 minutes after treatment in cells ectopically expressing WT TBK1, this effect was completely lost in cells expressing 2X K→R mutant TBK1 (Figure 4D and Figure S4D). Accordingly, quantitative analysis of confocal microscope images revealed significantly more pTBK1 puncta colocalizing with mitochondria in TBK1 knockout Huh7 cells transiently expressing WT TBK1 compared to cells expressing the 2X K→R mutant TBK1 following CCCP treatment (Figure 4E). In our mitochondrial fractionation experiments (Figure 4D and S4D), we saw a difference between WT TBK1 and 2X K→R mutant TBK1 in terms of their ability to facilitate the

recruitment of the autophagy machinery to damaged mitochondria. FIP200, ULK1 (both phosphorylated and total), and the autophagy adaptors Optineurin, SQSTM1, NDP52, and NBR1 were all enriched in mitochondrial fractions within 2 h after CCCP or ivermectin treatment in cells expressing WT TBK1. In contrast, these proteins' recruitment to damaged mitochondria was reduced or delayed in cells expressing 2X K→R mutant TBK1 (Figure 4D and S4D). We also observed more phosphorylation of the TBK1 substrate SQSTM1 in mitochondrial fractions from cells expressing WT TBK1 than in mitochondrial fractions from cells expressing 2X K→R (Figure 4D and Figure S4D). Taken together, these data demonstrate that mutation of the predominant ubiquitination sites on TBK1 abrogates the ability of TBK1 to become active on damaged mitochondria and subsequently enable the recruitment and activation of the rest of the autophagy machinery.

One way in which ubiquitination could increase TBK1 function is through facilitating the recruitment of TBK1 cofactors that mediate proper TBK1 localization or activation. Candidate cofactors include the autophagy adaptors SQSTM1, NDP52, Optineurin, TAX1BP1, and NBR1[25], all of which encode ubiquitin-binding domains. TBK1 ubiquitination by TRIM5α could promote these interactions and/or could contribute to the assembly of TBK1-adaptor clusters held together by avidity-based interactions. Accordingly, WT TBK1 more efficiently coimmunoprecipitates NBR1, NDP52, and SQSTM1 than does the ubiquitination deficient 2X K→R mutant of TBK1 (Figure 4F). We then tested whether mitochondrial damage with either CCCP or ivermectin, both of which induce TBK1 ubiquitination (Figure 3 and S3), could impact protein-protein interactions between TBK1 and autophagy adaptors, using NDP52 and NBR1 as representatives. We found that both treatments transiently increased the ability of myc-TBK1 to coimmunoprecipitate endogenous NDP52 and NBR1 (Figure 4G and Figure S4E). This effect was lost in TRIM5 knockout cells. Overall, these findings indicate that TRIM5α-dependent K63-linked ubiquitination of TBK1 is important for the formation of TBK1-adaptor protein complexes, possibly explaining the importance of this post-translational modification to TBK1-dependent mitophagy. To further test this model, we determined whether K63-linked poly-ubiquitin chains contribute to interactions between TBK1 and the autophagy adaptors NDP52, NBR1, and SQSTM1 by knocking down the e2 conjugating enzyme Ubc13/Ube2n, which is required for the formation of K63 linkages[49,50]. In Huh7 cells transfected with non-targeting siRNA, we saw that CCCP treatment increased the abundance of autophagy adaptors in protein complexes with TBK1, albeit with variable kinetics (Figure 4H). Knockdown of Ubc13 reduced the interactions between TBK1 and either NDP52 or SQSTM1 under basal conditions. Additionally, Ubc13 knockdown prevented any CCCP-induced increase in interactions between TBK1 and NDP52, NBR1, or SQSTM1. This experiment confirmed that K63-linked ubiquitin chains, likely deposited on TBK1 by TRIM5α, mediate TBK1 interactions with a subset of autophagy adaptors.

TRIM5α interacts with TBK1 through K63-linked poly-ubiquitin/autophagy adaptor intermediates.

In domain mapping experiments, we found that the TRIM5α RING domain was required for TRIM5α-TBK1 interactions in cells (Figure S5A, B). However, GST-pulldown experiments failed to show any interaction between recombinant TBK1 and either full-length TRIM5α

or the N terminal portion of TRIM5α (Figure S5C), indicating that TRIM5α-TBK1 interactions might require additional factors. Since the RING domain encompasses TRIM5α's ubiquitin ligase activity and is the site of TRIM5α auto-ubiquitination, it is possible that TRIM5α-mediated ubiquitination could contribute to TRIM5α-TBK1 interactions. In support of this concept, we observed that mitochondrial damaging agents increased the appearance of high molecular weight TRIM5α simultaneously with TRIM5α-TBK1 binding (Figure S1C). Both ivermectin and CCCP treatment dramatically increased TRIM5α ubiquitination in a time-dependent manner as measured by increases in the amount of ubiquitin coimmunoprecipitating with TRIM5α and the appearance of high molecular weight TRIM5α bands, the latter of which could represent either ubiquitinated TRIM5α and/or its organization into stabilized higher-order structures (Figure 5A and S5D). Follow-up experiments demonstrated that TRIM5α was subject to K63-linked ubiquitination in response to ivermectin and CCCP (Figure S5E, F). We found that the ivermectin-induced K63-linked poly-ubiquitination of TRIM5α is largely dependent on TRIM5α's ubiquitin ligase activity, since the E11R mutant of TRIM5α showed much less ubiquitination than did wild type (Figure 5B). This result demonstrates that TRIM5α is primarily auto-ubiquitinated, and that its ability to carry out auto-ubiquitination is enhanced following mitochondrial damage. However, we still observed ivermectin-induced K63-linked ubiquitination of TRIM5α E11R at 2 h after treatment, implicating additional ubiquitin ligases as secondary contributors to TRIM5α ubiquitination in response to mitochondrial damage (Figure 5B).

The increase in TRIM5α ubiquitination was mirrored by an increase in the interactions between TRIM5α and autophagy adaptors. As shown in Figure 5C, ivermectin treatment increased the ability of TRIM5α to coimmunoprecipitate endogenous NBR1, SQSTM1, and NDP52 within 30 minutes. The interaction between TRIM5α and SQSTM1 or NBR1 remained at high levels for at least the next 90 minutes; while with NDP52 interactions were dynamic, reproducibly showing strong binding at 30 minutes and variable binding at later time points. In transfected HEK293T cells, CCCP treatment also increased the interactions between TRIM5α and NDP52, optineurin, TAX1BP1, and NBR1 (Figure S5G–J) but not SQSTM1 (Figure S5K). Confocal microscopy experiments showed that TRIM5α and the autophagy adaptors NBR1, SQSTM1, and NDP52 colocalized in close proximity to Parkin-labeled mitochondria in CCCP-treated HeLa cells (Figure 5D). The interactions between TRIM5α and autophagy adaptors required ubiquitination, as knockdown of Ubc13 abrogates the ivermectin-induced interaction between TRIM5α and endogenous NDP52, NBR1, and SQSTM1 (Figure 5E). These data reveal previously unrecognized ubiquitin-dependent interactions between TRIM5α and autophagy adaptors that are responsive to mitochondrial damage.

We hypothesized that TRIM5α-TBK1 interactions could be mediated indirectly through shared interactions with autophagy adaptors. To test this, we determined whether TRIM5α and TBK1 could interact in cells lacking all five autophagy adaptors (PentaKO cells)[9]. As expected based on our prior experiments, both CCCP and ivermectin increased TRIM5α-TBK1 coimmunoprecipitation in WT HeLa cells. However, this increase was not seen in the PentaKO HeLa cells (Figure 5F, G and Figure S5L). This result demonstrates that one or more autophagy adaptors, all of which interact with both TRIM5α and TBK1[25], can scaffold

TRIM5α-TBK1 interactions. Given the role of TBK1 ubiquitination in its interactions with a subset of autophagy receptors (Figure 4), the importance of K63-linked ubiquitination in TRIM5α's interactions with autophagy adaptors, and the importance of autophagy adaptors in mediating TRIM5α-TBK1 interactions, we hypothesized that ubiquitination contributes to TRIM5α-TBK1 interactions. Accordingly, knockdown of Ubc13 prevented the time-dependent interactions between TRIM5α and both TBK1 and pTBK1 following mitochondrial damage with CCCP (Figure 5H). Deubiquitinase-fused TRIM5α was less efficient at interacting with TBK1 than was deubiquitinase-dead fused TRIM5α (Figure 5I), further emphasizing the importance of ubiquitination in TRIM5α-TBK1 interactions. Finally, we found that ubiquitinated residues K30 and K401 in TBK1 are contributors to TRIM5α-TBK1 interactions (Figure 5J), consistent with these residues' role in allowing interactions between TBK1 and autophagy adaptors (Figure 4G).

Our model for how TRIM5α and TBK1 interact in response to mitochondrial damage is shown in Figure 5K. Either CCCP or ivermectin enhance TRIM5α-mediated K63-linked ubiquitination of itself and of TBK1. Ubiquitin chains attached to either TRIM5α or TBK1 or both then attract autophagy adaptors, which can then further bridge TRIM5α and TBK1 through shared interactions. In this way, TRIM5α can promote the condensation, concentration, and subsequent activation of TBK1 and autophagy adaptors on the mitochondria through self-amplifying multivalent interactions, thus laying a foundation for the recruitment of the autophagy machinery.

TRIM5α cooperates with TRIM27 in executing mitophagy.

In addition to TRIM5α's role in ubiquitin-dependent mitophagy, we showed that another TRIM, TRIM27 (also known as Ret finger protein, RFP), contributes to ubiquitin-independent mitophagy mediated by FKBP8 and promotes the mitochondrial localization of pTBK1[51]. TRIM5α and TRIM27 are closely related genes[32], raising the possibility that these TRIMs employ overlapping mechanisms in mitophagy. In support of this concept, we found that ectopic expression of GFP-TRIM27 was just as efficient at restoring CCCP-induced mitophagy in TRIM5 knockout Huh7 cells as was expression of GFP-TRIM5α (Figure 6A). Analysis of TRIM5α interacting partners suggested possible interactions with TRIM27[31], which we confirmed by coimmunoprecipitation experiments (Figure 6B). TRIM5α-HA and GFP-TRIM27 colocalize in cytoplasmic structures observed by confocal microscopy in HeLa cells (Figure S6A). Importantly, TRIM5α/TRIM27-double positive puncta colocalized at discreet sub-domains of mCherry-Parkin-positive mitochondria (Figure 6C), positioning them to have similar functions in mitophagy. Ivermectin treatment increased the formation of TRIM5α-TRIM27 protein complexes (Figure 6D), showing that TRIM27 is recruited into TRIM5α complexes under mitophagy-inducing conditions. Finally, TRIM5α-HA was better able to coimmunoprecipitate myc-TBK1 in invermectin-treated cells expressing GFP-TRIM27 than in ivermectin-treated cells expressing GFP-alone (Figure 6E). Together, these studies demonstrate that TRIM27 promotes TRIM5α- and ubiquitin-dependent mitophagy, likely through actions focused on TBK1. In conclusion, our studies with TRIM5α and TRIM27 provide a model for how TRIM-directed mitophagy functions.

DISCUSSION

The molecular events leading up to mitophagy involve the concerted recruitment of multiple individual proteins and protein complexes to the mitochondria, often as part of feed-forward loops that rapidly amplify the local concentration of mitophagy factors and induce their activation. Our study shows that TRIM5α, and potentially other TRIMs like TRIM27, are essential initiators of this cascade. Mitochondrial stress activates TRIM5α's enzymatic activity, resulting in K63-linked auto-ubiquitination. These ubiquitin chains serve as scaffolds that link TRIM5α with ubiquitin-binding autophagy adaptor proteins (e.g. NDP52, Optineurin, p62/SQSTM1, NBR1, and TAX1BP1). All of these adaptor proteins also interact with TBK1, and they serve as intermediaries that bridge TRIM5α-TBK1 interactions. This allows TRIM5α to catalyze K63-linked ubiquitination of TBK1 at K30 and K401, promoting TBK1 activity while also providing additional landing sites for autophagy adaptor recruitment and subsequent assembly of TRIM5α-ubiquitin-TBK1 complexes in a self-amplifying manner.

This TRIM-ubiquitin-TBK1 axis is required for the proper activation and localization of TBK1 in mitophagy. K63-linked ubiquitination of TBK1 is essential for TBK1 activity in immune signaling[46,47], and our studies have extended this to TBK1's functions in selective autophagy. We found that TBK1 ubiquitination is increased in response to mitochondrial damage in a TRIM5α-dependent manner. A TBK1 mutant that shows reduced ubiquitination (2X K→R) is defective in restoring mitophagy in TBK1 knockout cells, and multiple lines of evidence suggest that TBK1 ubiquitination by TRIM5α is necessary for TBK1 to interact with a subset of autophagy adaptors in response to mitochondrial damaging agents. By promoting interactions between autophagy adaptors and TBK1, TRIM5α enables the concentration of TBK1 on damaged mitochondria, resulting in TBK1 activation. Active TBK1 can phosphorylate autophagy adaptors near their ubiquitin-binding domains, promoting the adaptors' ability to interact with ubiquitinated TRIM5α, TBK1, or mitochondrial proteins[27]. Phosphorylation of autophagy adaptors by TBK1 enhances the adaptors' ability to interact with and recruit the ULK1/FIP200 complex or LC3 and GABARAP proteins[8,52]. TBK1 can also promote mitophagy through phosphorylation of RAB7A[53] or by directly activating the phosphatidylinositol 3-kinase (PI3K) complex I[29]. By activating TBK1, TRIM5α is upstream of all of these processes.

A key difference between the actions of TRIM5α that we report here and the actions of Parkin or other E3 ligases previously implicated in mitophagy is in the nature of the ubiquitinated targets. In Parkin-dependent mitophagy, Parkin ubiquitylates a wide variety of proteins on the mitochondrial outer membrane[54], allowing for the recruitment of autophagy adaptors[9]. In contrast, TRIM5α appears to ubiquitylate itself and TBK1. As is the case with Parkin-dependent mitophagy, this will allow the assembly of autophagy adaptor-TBK1 complexes where they are needed when mitochondria are damaged. However, in order for TBK1 to become activated, it must be attached to K63-linked poly-ubiquitin chains at lysine residues 30 and 401[47]. This additional level of mitophagy regulation is provided by TRIM5α.

Our data show that additional TRIMs are also involved in mediating mitophagy through actions on TBK1. TRIM27 shows substantial homology to TRIM5α, and we previously reported that TRIM27 contributes to an ubiquitin-independent form of mitophagy[51]. Here, we showed that TRIM27 expression can rescue mitophagy in TRIM5 knockout cells. This, along with the strong colocalization of TRIM5α and TRIM27 on the surface of mitochondria following damage suggests that TRIM5α and TRIM27 operate through overlapping mechanisms to execute mitophagy. However, the finding that TRIM27 could enhance TRIM5α interactions with TBK1 in response to mitochondrial damage suggests that these two proteins may not be fully redundant. More study is necessary to address whether TRIM27 uses the same mechanism(s) as does TRIM5α in mitophagy or to determine if there are cell type- or context-dependent differences between mitophagy mediated by these two TRIMs.

Both TRIM5α and TBK1 are best appreciated for their roles in antiviral defense and innate immunity. Mitochondria likely evolved from intracellular bacterial parasites, and molecules released from damaged mitochondria can activate pathogen-associated molecular pattern receptors[23]. Thus, our finding that TRIM5α and TBK1 work together in mitochondrial quality control is in agreement with their immunological functions. The mechanisms employed by TRIM5α in mitophagy parallel its functions in retroviral restriction (Figure 6F), as exemplified by the rhesus TRIM5α/HIV-1 model[35]. Rhesus TRIM5α assembles into higher-order structures on assembled HIV-1 core structures[55]. This induces TRIM5α's ubiquitin ligase activity, leading to the ubiquitin-dependent activation of the kinase TAK1 and subsequent establishment of an antiviral state[44]. Similarly, here we showed that TRIM5α assembles higher-order structures consisting of itself, TBK1, and autophagy adaptors on damaged mitochondria. This assembly is associated with an increase in TRIM5α's ubiquitin ligase activity, which leads to the ubiquitin-dependent activation of the kinase TBK1 and subsequent activation of mitophagy. In response to the threat of either retroviral infection or mitochondrial damage, TRIM5α plays a cytoprotective role.

In conclusion, our study positions TRIMs at a central node in mitophagy regulation (Figure S6B), from which they can orchestrate mitophagy through regulating the activation and localization of TBK1. In addition to TRIM5α and TRIM27, many other TRIMs have been implicated in regulating selective autophagy of a variety of substrates[56]. The TRIM-ubiquitin-TBK1 axis provides a new lens through which the mechanistic basis for selective autophagy by other TRIMs could be viewed.

Limitations of the study

In this study, we determined the mechanisms of TRIM5α-mediated mitophagy in immortalized cancer cell lines. We found that chemical agents that damage mitochondria and induce mitophagy increase TRIM5α-mediated ubiquitination of itself and of TBK1, but we have not identified how mitochondrial damage is translated into activation of TRIM5α's enzymatic activity. Presumably, this involves the higher-order assembly of TRIM5α molecules as is seen by TRIM5α in the context of retroviral capsid recognition[43] or by TRIM72 in response to recognition of vesicle structures[57]. Using a broad array of coimmunoprecipitation assays, we established that TRIM5α and TBK1 likely interact

indirectly in a manner requiring K63-linked poly-ubiquitin chains and autophagy adaptors, but efforts to predict how these interactions form on a structural level using AlphaFold[58] or structural docking software[59] failed to yield high-confidence models. We also did not determine the relative importance of the five autophagy adaptors in mediating TRIM5α/TBK1 interactions.

STAR METHODS

RESOURCE AVAILABILITY

Lead contact—Further information and requests for reagents should be directed to and will be fulfilled by the lead contact, Mike Mandell (mmandell@salud.unm.edu).

Materials availability—Plasmids or cell lines generated in this study are available upon request to the lead contact.

Data and code availability—All data reported in this paper will be shared by the lead contact upon request. This paper does not report original code. Any additional information required to reanalyze the data reported in this paper is available from the lead contact upon request.

EXPERIMENTAL MODEL

Cell culture—HEK293T, HeLa, and Huh7 cells were obtained from the American Type Culture Collection (ATCC) and grown in Dulbecco's modified Eagle's medium (Life Technologies,11965126) supplemented with 10% fetal bovine serum (FBS, Life technologies, 26140–079), 100 U/ml penicillin and 100 μg/ml streptomycin at 37°C in a 5% CO2 atmosphere. HeLa cells stably expressing HA-tagged HuTRIM5α were obtained from Joseph Sodroski (Harvard) and were maintained in the above media supplemented with 1 μg/ml puromycin. Generation of TRIM5 knockout HEK293T, HeLa, and Huh7 cells using CRISPR/Cas9 based gene editing were described previously[31] and were maintained in the above media supplemented with 200 μg/ml hygromycin. WT and mitophagy adaptor pentaKO cells (gifts from Dr. Richard J. Youle, National Institutes of Health, USA), were cultured in the same manner. TBK1 knockout HEK293T and TRIM5-TBK1 double knockout Huh7 cells were generated by transduction with lentiCRISPRv2-based lentiviruses followed by 2–4 weeks of culturing in medium containing 8 μg/ml blasticidin. Knockout lines were confirmed by immunoblot. Mt-mkeima stable overexpression in Huh7 WT, Huh7 TRIM5 KO and Huh7 TBK1 KO lines were achieved by viral transduction followed by 14–21 days of culturing in medium containing the selective antibiotic (1 μg/ml puromycin).

METHOD DETAILS

Generation of knockout cell lines using CRISPR/cas9 gene editing—Viral particles for the generation of knockout cell lines were produced by transfecting HEK293T cells with a lentiviral vector, lentiCRISPRv2 carrying both Cas9 enzyme and a guide RNA targeting specific gene together with the packaging plasmids psPAX2 and pMD2.G at the ratio of 10 μg, 10 μg and 10 μg/10 cm dish. Transfections were carried out by using ProFection Mammalian Transfection System (Promega, E1200), medium was changed 16h

post transfection and virus containing supernatant was harvested 48h later, clarified by centrifuging for 5 min at 1200 rpm, 0.45 μm-filtered (Millipore, SE1M003M00), diluted with full medium at 1:1 ratio and used to transduce target cells for 48 h.

Cloning and transfection—GFP-TRIM5α and myc-TBK1 were mutated using a site-directed mutagenesis kit (Agilent, 210518). All plasmid constructs generated in this study were validated by DNA sequencing. All other TRIM5α mutants used in this study were described earlier[60]. Myc-TBK1 and FLAG- tagged autophagy adaptor plasmids were gift from Dr. Vojo Deretic. The NF-κB luciferase reporter was purchased from Promega (#E8491), the Renilla luciferase plasmid (pRL-SV40, Addgene plasmid #27163) was a gift from Ron Prywes and ISRE luciferase plasmid was gifted by Dr. Michael Gale (University of Washington). Dub-TRIM5α (rhesus) and Dub*-TRIM5α were a gift from Dr. Edward Campbell. pDest-EGFP-TRIM27 was described earlier[51]. pDONR221-AZI2/NAP1 was synthesized by Invitrogen GeneArt services (Thermo Fisher Scientific). pDest15-AZI2/NAP1 was made with Gateway LR cloning (Thermo Fisher Scientific). pDest15-TRIM5α plasmids were also constructed using Gateway cloning. Plasmid transfections were performed using Lipofectamine 2000 (ThermoFisher, 11668019) or Calcium Phosphate (Promega, E1200). Samples were prepared for analysis the day after DNA transfection.

All siRNA smart pools were from Dharmacon. siRNA was delivered to cells using Lipofectamine RNAiMAX (ThermoFisher, 13778150) according to the manufacturer'. For siRNA experiments, cells were harvested 48–72h after siRNA transfection.

Treatments—Working concentrations for reagents were as follows: CCCP, 10 μM for overnight experiments; and 20 μM for experiments ≤ 4 hours; IVM, 15 μM; BX-795, 10 μM; 5Z-7-Oxozeaenol, 10 μM; pp242, 10 μM; LLOMe, 100 μM; MG132, 10 μM; PhenoVue 641 mitochondrial stain, 300 nM.

Mitophagy assays—*Flow cytometry-based mito-mKeima mitophagy assay*. Cells were seeded in six well plates one day prior to treatment or transient transfection. Following mitophagy induction with 20 μM ivermectin for 6 hours, cells were washed with PBS, detached with trypsin and harvested in normal growth media. Samples were then centrifuged at 4^{o} C, washed once with PBS and then resuspended in ice cold FACS buffer (PBS+2% FBS).

Measurements of mt-mKeima were made using dual-excitation ratiometric pH measurements at 440nm (pH 7) and 585nm (pH 4) lasers. The emission wavelength for mt-mKeima is identical at either pH and peaks maximally at 620 nm. Sample analysis was performed using an Attune NxT flow cytometer (Thermofisher). For each sample, 50,000 events were collected. Data were analyzed using FlowJo (v10.10.0).

Immunoblot-based measurement of mitochondrial protein degradation. Huh7 TRIM5 KO and Huh7 TBK1 KO cell lines were seeded in 6 cm dishes, followed by transfection on next day with the indicated plasmids. Cells were then treated with 10 μM CCCP for 18 hours and conducted western blot analysis of several different mitochondrial proteins.

Western blotting, immunoprecipitation, and immunofluorescent labeling—For immunoprecipitation experiments, cells seeded in 10 cm dishes were transfected with specific constructs to overexpress proteins of interest for 24 h, followed by the indicated treatments in the presence of MG132. Cells were then lysed using ice cold lysis buffer (150 mM Tris-buffered Saline, 50 mM NaCl, with 0.5% v/v Triton-X 100) supplemented with EDTA-free cOmplete protease inhibitor, PMSF, and phosphatase inhibitors. Samples were incubated on ice for 30 min. Beads were equilibrated using the lysis buffer mentioned above. Protein lysates were precleared by centrifugation at 4°C for 15 min at 17,000 g. Clarified lysates were incubated with specific equilibrated beads for various periods at 4°C. Beads were then washed with ice cold Wash buffer (150 mM Tris-buffered Saline, 50 mM NaCl) 3 to 4 times. Bound proteins were eluted with LDS lysis buffer with 50 mM DTT. Samples were boiled for an additional 10 min. For ubiquitination related immunoprecipitation experiments, a deubiquitinase inhibitor (PR-619; 10 μM, UBPBio) was added in lysis buffer and in wash buffers in addition to the protease inhibitors detailed above. For these experiments, we lysed cells in RIPA buffer (50 mm Tris, 0.1% SDS, 0.5% deoxycholate, 1% Nonidet P-40, 150 mM NaCl) to reduce non-covalent interactions between proteins and ubiquitin.

SDS PAGE was carried out using pre-cast poly-acrylamide gels (Biorad) and immunoblotted on nitrocellulose membranes. After transfer, blots were blocked in 5% non-fat powder milk dissolved in 1X PBS prior to overnight incubations in primary antibodies diluted in a bugger containing 3% BSA and 0.1% Tween-20 in 1X PBS. Immunoblot data was acquired using a Chemidoc MP instrument (Biorad) and quantitatively analyzed using Biorad Image Lab software.

For immunoflourescent labeling of samples for high content imaging or confocal experiments, samples were fixed in 4% paraformaldehyde (Sigma) for 30 minutes prior to permeabilization in buffer containing 0.1% Saponin (Sigma) and 3% BSA. Following 1 hour incubation in primary antibodies and extensive washing with phosphate buffered saline (PBS), AlexaFluor-conjugated secondary antibodies (Life Technologies) were used. Coverslips were mounted in ProLong Diamond anti-fade reagent (Life Technologies).

Denaturing IP—Denaturing immunoprecipitation was performed as previously described[61]. Cell pellets from transiently transfected TRIM5 knockout HEK293T cells were harvested by centrifugation and then resuspended in RIPA lysis buffer supplemented with 1% SDS and deubiquitinase inhibitors (PR619; 10 μM and 1, 10- phenanthroline monohydrate: 1mM) for 30 minutes. Samples were then boiled at 95°C for 10 min and passaged through a 25 g needle attached to a 1-ml syringe until the solution was clear. Cell lysates were then clarified by centrifugation. The supernatant was then diluted with 10 volumes RIPA lysis buffer to reduce the SDS concentration to 0.1% prior to immunoprecipitation following our standard procedures.

Confocal microscopy—Sub-airy unit (0.6AU) pinhole confocal microscopy with a Leica TCS-SP8 microscope was performed followed by computational image restoration with Huygens Essential (Scientific Volume Imaging, Hilversum, Netherlands) utilizing a constrained maximum likelihood estimation algorithm. All images were acquired with

a 63X/1.4NA plan apochromat oil immersion objective and sampled at ideal Nyquist sampling rates in x, y, and z planes. Voxel lateral and axial dimensions were determined by utilizing an online Nyquist calculator (https://svi.nl/NyquistCalculator) allowing for sub-diffraction limited resolution following image restoration. All images were rendered on a high performance CUDA-GPU enabled workstation. 3D projections were generated using the Surface Renderer application in the Huygens software. The Object Analyzer application in the Huygens software was used to determine the relative colocalization between objects in three dimensions. To do this, 3D objects were identified and segmented in the Huygens software based on uniformly applied threshold settings. These objects were defined as regions of interest (ROI). The "Intensity in the other channel" functionality was then used to quantitate the total fluorescent signal intensity from other channels within the ROI. Relative colocalization was determined by dividing the signal intensity from one channel (e.g. pTBK1) within the ROI by the volume of the ROI (e.g. mitochondria).

Proximity ligation assay—Proximity ligation assay (PLA) was performed according to manufacturer instructions (Millipore). PLA reports direct *in situ* interactions between proteins that are within 40nm of each other and revealed as fluorescent dots.

High content imaging—All high content experiments were performed on Huh7 cells in 96-well plate format using optical-quality glass-bottomed plates. Imaging and analysis were performed using a Cellomics CellInsight CX7 scanner and driven by iDEV software (Thermo Fisher Scientific). Primary objects (cells, identified based on nuclear staining with Hoechst 33342 and regions of interest (ROI) were algorithm-defined by shape/segmentation, maximum/minimum average intensity, total area and total intensity to automatically identify puncta within valid primary objects. Five wells (>1000 cells/well) were analyzed per treatment per experiment. All data acquisition and analysis were computer driven and independent of human operators.

Mitochondrial isolation experiments—Subcellular fractionation was performed with a QProteome mitochondria isolation kit (Qiagen) according to the instruction manual. In brief, 10^7 Huh7 and HeLa cells were re-suspended in 1 mL of lysis buffer, incubated for 10 min at 4^o C and centrifuged at 1000x g for 10 min. The supernatant was transferred into a separate tube as cytosolic fraction, while the pellet was re-suspended in 1.5 mL of ice-cold disruption buffer, rapidly passed through 26g needle 10–15 times to disrupt cells and centrifuged at 1000x g for 10 min, 4^o C. The supernatant was then re-centrifuged at 6000x g for 10 min, 4^o C. The pellet obtained after centrifugation comprised the mitochondrial fraction.

Luciferase assays—20000 HEK293T cells were plated in 96 well plates prior to transfection with the *Renilla* luciferase internal control reporter plasmid pRL-TK (thymidine kinase promoter dependent *Renilla* luciferase), plasmids encoding firefly luciferase responsive to NF-κB or ISRE and GFP, GFP-TRIM5α with or without myc-TBK1 expression plasmids. 40–48h after transfection, the plate was assayed using the Dual-Glo Luciferase Assay System according to the manufacturer's instructions (Promega, E2920) and read using a Microplate Luminometer (BioTek, SYNERGY HTX Multi-Mode reader). Firefly luciferase readings were normalized to Renilla luciferase readings in each well, and

the data are represented as fold-change relative to GFP alone. Each experimental condition was performed in quadruplicate.

GST pull-down assays—GST pulldown assays were performed by incubating immobilized GST or GST-tagged proteins with ^{35}S-labeled *in vitro* translated proteins. All GST-tagged proteins were expressed in *Escherichia coli* SoluBL21 (Genlantis). GST fusion proteins were purified on glutathione-Sepharose 4 Fast Flow beads (GE Healthcare 17-5132-01). ^{35}S-labeled proteins were synthesized *in vitro* using the TnT T7 coupled reticulocyte lysate system (Promega). Translation reaction products from 0.25 μg of plasmid DNA were incubated with GST-labeled proteins on glutathione-Sepharose beads in NETN-E buffer (50 mM Tris, pH 8.0, 100 mM NaCl, 1 mM EDTA, 0.5% Nonidet P-40) supplemented with cOmplete Mini EDTA-free protease inhibitor cocktail tablets (1 tablet/10ml) (11836170001, Roche) for 1 h at 4°C. The beads were washed five times with 400 μl of NETN-E buffer, boiled with 2× SDS-PAGE gel loading buffer with 1mM DTT, and subjected to SDS-PAGE. Gels were stained with Coomassie Brilliant Blue and vacuum-dried. ^{35}S-labeled proteins were detected using a Fujifilm bioimaging analyzer BAS-5000 (Fuji) and quantifications were performed using Image Gauge software (Fuji).

QUANTIFICATION AND STATISTICAL ANALYSIS

Data are expressed as means ± SEM (n>3). Data were analyzed with unpaired two-tailed t-tests or ANOVA with Tukey's post hoc analysis as indicated in the figure legends. Analysis was performed using GraphPad Prism10. Statistical significance is defined as *, $P < 0.05$; **, $P < 0.01$; ***, $P < 0.001$; ****, $P < 0.0001$.

Supplementary Material

Refer to Web version on PubMed Central for supplementary material.

Acknowledgements

This work was supported by P20GM121176 and R01AI155746 to M.A.M and T32AI007538 to S.O. from the US National Institutes of Health. Confocal microscopy and flow cytometry were performed in the University of New Mexico Comprehensive Center, which are supported by P30CA118100 form the NIH. Dr. Ed Campbell (Loyola University Chicago) shared the TRIM5α deubiquitinase plasmids. Dr. Richard Youle (NIH) shared the PentaKO cells. Dr. Ruheena Javed (University of New Mexico) and Dr. Santosh Chauhan (CSIR India-CCMB) commented on the manuscript. Biorender software was used to generate graphics.

References:

1. Pickles S, Vigie P, and Youle RJ (2018). Mitophagy and Quality Control Mechanisms in Mitochondrial Maintenance. Curr Biol 28, R170–R185. 10.1016/j.cub.2018.01.004. [PubMed: 29462587]
2. Onishi M, Yamano K, Sato M, Matsuda N, and Okamoto K (2021). Molecular mechanisms and physiological functions of mitophagy. The EMBO journal 40, e104705. 10.15252/embj.2020104705. [PubMed: 33438778]
3. Pickrell AM, Huang CH, Kennedy SR, Ordureau A, Sideris DP, Hoekstra JG, Harper JW, and Youle RJ (2015). Endogenous Parkin Preserves Dopaminergic Substantia Nigral Neurons following Mitochondrial DNA Mutagenic Stress. Neuron 87, 371–381. 10.1016/j.neuron.2015.06.034. [PubMed: 26182419]

4. Evans CS, and Holzbaur ELF (2019). Autophagy and mitophagy in ALS. Neurobiology of disease 122, 35–40. 10.1016/j.nbd.2018.07.005. [PubMed: 29981842]
5. Gong G, Song M, Csordas G, Kelly DP, Matkovich SJ, and Dorn GW 2nd (2015). Parkin-mediated mitophagy directs perinatal cardiac metabolic maturation in mice. Science 350, aad2459. 10.1126/science.aad2459.
6. Uoselis L, Nguyen TN, and Lazarou M (2023). Mitochondrial degradation: Mitophagy and beyond. Molecular cell. 10.1016/j.molcel.2023.08.021.
7. Bunker EN, Le Guerroue F, Wang C, Strub MP, Werner A, Tjandra N, and Youle RJ (2023). Nix interacts with WIPI2 to induce mitophagy. The EMBO journal, e113491. 10.15252/embj.2023113491. [PubMed: 37621214]
8. Vargas JNS, Wang C, Bunker E, Hao L, Maric D, Schiavo G, Randow F, and Youle RJ (2019). Spatiotemporal Control of ULK1 Activation by NDP52 and TBK1 during Selective Autophagy. Molecular cell 74, 347–362 e346. 10.1016/j.molcel.2019.02.010. [PubMed: 30853401]
9. Lazarou M, Sliter DA, Kane LA, Sarraf SA, Wang C, Burman JL, Sideris DP, Fogel AI, and Youle RJ (2015). The ubiquitin kinase PINK1 recruits autophagy receptors to induce mitophagy. Nature 524, 309–314. 10.1038/nature14893. [PubMed: 26266977]
10. Hung CM, Lombardo PS, Malik N, Brun SN, Hellberg K, Van Nostrand JL, Garcia D, Baumgart J, Diffenderfer K, Asara JM, and Shaw RJ (2021). AMPK/ULK1-mediated phosphorylation of Parkin ACT domain mediates an early step in mitophagy. Science advances 7. 10.1126/sciadv.abg4544.
11. Wei Y, Chiang WC, Sumpter R Jr., Mishra P, and Levine B (2017). Prohibitin 2 Is an Inner Mitochondrial Membrane Mitophagy Receptor. Cell 168, 224–238 e210. 10.1016/j.cell.2016.11.042. [PubMed: 28017329]
12. Princely Abudu Y, Pankiv S, Mathai BJ, Hakon Lystad A, Bindesboll C, Brenne HB, Yoke Wui Ng M, Thiede B, Yamamoto A, Mutugi Nthiga T, et al. (2019). NIPSNAP1 and NIPSNAP2 Act as "Eat Me" Signals for Mitophagy. Developmental cell 49, 509–525 e512. 10.1016/j.devcel.2019.03.013. [PubMed: 30982665]
13. Abudu YP, Shrestha BK, Zhang W, Palara A, Brenne HB, Larsen KB, Wolfson DL, Dumitriu G, Oie CI, Ahluwalia BS, et al. (2021). SAMM50 acts with p62 in piecemeal basal- and OXPHOS-induced mitophagy of SAM and MICOS components. The Journal of cell biology 220. 10.1083/jcb.202009092.
14. Heo JM, Ordureau A, Paulo JA, Rinehart J, and Harper JW (2015). The PINK1-PARKIN Mitochondrial Ubiquitylation Pathway Drives a Program of OPTN/NDP52 Recruitment and TBK1 Activation to Promote Mitophagy. Molecular cell 60, 7–20. 10.1016/j.molcel.2015.08.016. [PubMed: 26365381]
15. Kane LA, Lazarou M, Fogel AI, Li Y, Yamano K, Sarraf SA, Banerjee S, and Youle RJ (2014). PINK1 phosphorylates ubiquitin to activate Parkin E3 ubiquitin ligase activity. The Journal of cell biology 205, 143–153. 10.1083/jcb.201402104. [PubMed: 24751536]
16. Harper JW, Ordureau A, and Heo JM (2018). Building and decoding ubiquitin chains for mitophagy. Nature reviews. Molecular cell biology 19, 93–108. 10.1038/nrm.2017.129. [PubMed: 29358684]
17. Zachari M, Gudmundsson SR, Li Z, Manifava M, Cugliandolo F, Shah R, Smith M, Stronge J, Karanasios E, Piunti C, et al. (2019). Selective Autophagy of Mitochondria on a Ubiquitin-Endoplasmic-Reticulum Platform. Developmental cell 50, 627–643 e625. 10.1016/j.devcel.2019.06.016. [PubMed: 31353311]
18. Turco E, Witt M, Abert C, Bock-Bierbaum T, Su MY, Trapannone R, Sztacho M, Danieli A, Shi X, Zaffagnini G, et al. (2019). FIP200 Claw Domain Binding to p62 Promotes Autophagosome Formation at Ubiquitin Condensates. Molecular cell 74, 330–346 e311. 10.1016/j.molcel.2019.01.035. [PubMed: 30853400]
19. Ravenhill BJ, Boyle KB, von Muhlinen N, Ellison CJ, Masson GR, Otten EG, Foeglein A, Williams R, and Randow F (2019). The Cargo Receptor NDP52 Initiates Selective Autophagy by Recruiting the ULK Complex to Cytosol-Invading Bacteria. Molecular cell 74, 320–329 e326. 10.1016/j.molcel.2019.01.041. [PubMed: 30853402]

20. Moehlman AT, Kanfer G, and Youle RJ (2023). Loss of STING in parkin mutant flies suppresses muscle defects and mitochondria damage. PLoS genetics 19, e1010828. 10.1371/journal.pgen.1010828. [PubMed: 37440574]
21. Rai P, Janardhan KS, Meacham J, Madenspacher JH, Lin WC, Karmaus PWF, Martinez J, Li QZ, Yan M, Zeng J, et al. (2021). IRGM1 links mitochondrial quality control to autoimmunity. Nature immunology 22, 312–321. 10.1038/s41590-020-00859-0. [PubMed: 33510463]
22. Xu Y, Shen J, and Ran Z (2020). Emerging views of mitophagy in immunity and autoimmune diseases. Autophagy 16, 3–17. 10.1080/15548627.2019.1603547. [PubMed: 30951392]
23. Marchi S, Guilbaud E, Tait SWG, Yamazaki T, and Galluzzi L (2023). Mitochondrial control of inflammation. Nature reviews. Immunology 23, 159–173. 10.1038/s41577-022-00760-x.
24. Louis C, Burns C, and Wicks I (2018). TANK-Binding Kinase 1-Dependent Responses in Health and Autoimmunity. Frontiers in immunology 9, 434. 10.3389/fimmu.2018.00434. [PubMed: 29559975]
25. Zellner S, Schifferer M, and Behrends C (2021). Systematically defining selective autophagy receptor-specific cargo using autophagosome content profiling. Molecular cell 81, 1337–1354 e1338. 10.1016/j.molcel.2021.01.009. [PubMed: 33545068]
26. Moore AS, and Holzbaur EL (2016). Dynamic recruitment and activation of ALS-associated TBK1 with its target optineurin are required for efficient mitophagy. Proceedings of the National Academy of Sciences of the United States of America 113, E3349–3358. 10.1073/pnas.1523810113. [PubMed: 27247382]
27. Richter B, Sliter DA, Herhaus L, Stolz A, Wang C, Beli P, Zaffagnini G, Wild P, Martens S, Wagner SA, et al. (2016). Phosphorylation of OPTN by TBK1 enhances its binding to Ub chains and promotes selective autophagy of damaged mitochondria. Proceedings of the National Academy of Sciences of the United States of America 113, 4039–4044. 10.1073/pnas.1523926113. [PubMed: 27035970]
28. Pilli M, Arko-Mensah J, Ponpuak M, Roberts E, Master S, Mandell MA, Dupont N, Ornatowski W, Jiang S, Bradfute SB, et al. (2012). TBK-1 promotes autophagy-mediated antimicrobial defense by controlling autophagosome maturation. Immunity 37, 223–234. 10.1016/j.immuni.2012.04.015. [PubMed: 22921120]
29. Nguyen TN, Sawa-Makarska J, Khuu G, Lam WK, Adriaenssens E, Fracchiolla D, Shoebridge S, Bernklau D, Padman BS, Skulsuppaisarn M, et al. (2023). Unconventional initiation of PINK1/Parkin mitophagy by Optineurin. Molecular cell 83, 1693–1709 e1699. 10.1016/j.molcel.2023.04.021. [PubMed: 37207627]
30. Ma X, Helgason E, Phung QT, Quan CL, Iyer RS, Lee MW, Bowman KK, Starovasnik MA, and Dueber EC (2012). Molecular basis of Tank-binding kinase 1 activation by transautophosphorylation. Proceedings of the National Academy of Sciences of the United States of America 109, 9378–9383. 10.1073/pnas.1121552109. [PubMed: 22619329]
31. Saha B, Salemi M, Williams GL, Oh S, Paffett ML, Phinney B, and Mandell MA (2022). Interactomic analysis reveals a homeostatic role for the HIV restriction factor TRIM5alpha in mitophagy. Cell reports 39, 110797. 10.1016/j.celrep.2022.110797. [PubMed: 35545034]
32. Short KM, and Cox TC (2006). Subclassification of the RBCC/TRIM superfamily reveals a novel motif necessary for microtubule binding. The Journal of biological chemistry 281, 8970–8980. 10.1074/jbc.M512755200. [PubMed: 16434393]
33. Stremlau M, Owens CM, Perron MJ, Kiessling M, Autissier P, and Sodroski J (2004). The cytoplasmic body component TRIM5alpha restricts HIV-1 infection in Old World monkeys. Nature 427, 848–853. 10.1038/nature02343 nature02343 [pii]. [PubMed: 14985764]
34. Koepke L, Gack MU, and Sparrer KM (2021). The antiviral activities of TRIM proteins. Current opinion in microbiology 59, 50–57. 10.1016/j.mib.2020.07.005. [PubMed: 32829025]
35. Ganser-Pornillos BK, and Pornillos O (2019). Restriction of HIV-1 and other retroviruses by TRIM5. Nature reviews. Microbiology 17, 546–556. 10.1038/s41579-019-0225-2. [PubMed: 31312031]
36. Zhao Y, Lu Y, Richardson S, Sreekumar M, Albarnaz JD, and Smith GL (2023). TRIM5alpha restricts poxviruses and is antagonized by CypA and the viral protein C6. Nature 620, 873–880. 10.1038/s41586-023-06401-0. [PubMed: 37558876]

37. Chiramel AI, Meyerson NR, McNally KL, Broeckel RM, Montoya VR, Mendez-Solis O, Robertson SJ, Sturdevant GL, Lubick KJ, Nair V, et al. (2019). TRIM5alpha Restricts Flavivirus Replication by Targeting the Viral Protease for Proteasomal Degradation. Cell reports 27, 3269–3283 e3266. 10.1016/j.celrep.2019.05.040. [PubMed: 31189110]

38. Yamada Y, Yasukochi Y, Kato K, Oguri M, Horibe H, Fujimaki T, Takeuchi I, and Sakuma J (2018). Identification of 26 novel loci that confer susceptibility to early-onset coronary artery disease in a Japanese population. Biomed Rep 9, 383–404. 10.3892/br.2018.1152. [PubMed: 30402224]

39. van der Harst P, and Verweij N (2018). Identification of 64 Novel Genetic Loci Provides an Expanded View on the Genetic Architecture of Coronary Artery Disease. Circulation research 122, 433–443. 10.1161/CIRCRESAHA.117.312086. [PubMed: 29212778]

40. Yamada Y, Kato K, Oguri M, Horibe H, Fujimaki T, Yasukochi Y, Takeuchi I, and Sakuma J (2018). Identification of 13 novel susceptibility loci for early-onset myocardial infarction, hypertension, or chronic kidney disease. International journal of molecular medicine 42, 2415–2436. 10.3892/ijmm.2018.3852. [PubMed: 30226566]

41. Aragam KG, Jiang T, Goel A, Kanoni S, Wolford BN, Atri DS, Weeks EM, Wang M, Hindy G, Zhou W, et al. (2022). Discovery and systematic characterization of risk variants and genes for coronary artery disease in over a million participants. Nature genetics 54, 1803–1815. 10.1038/s41588-022-01233-6. [PubMed: 36474045]

42. Wong YC, and Holzbaur EL (2014). Optineurin is an autophagy receptor for damaged mitochondria in parkin-mediated mitophagy that is disrupted by an ALS-linked mutation. Proceedings of the National Academy of Sciences of the United States of America 111, E4439–4448. 10.1073/pnas.1405752111. [PubMed: 25294927]

43. Fletcher AJ, Vaysburd M, Maslen S, Zeng J, Skehel JM, Towers GJ, and James LC (2018). Trivalent RING Assembly on Retroviral Capsids Activates TRIM5 Ubiquitination and Innate Immune Signaling. Cell host & microbe 24, 761–775 e766. 10.1016/j.chom.2018.10.007. [PubMed: 30503508]

44. Pertel T, Hausmann S, Morger D, Zuger S, Guerra J, Lascano J, Reinhard C, Santoni FA, Uchil PD, Chatel L, et al. (2011). TRIM5 is an innate immune sensor for the retrovirus capsid lattice. Nature 472, 361–365. 10.1038/nature09976. [PubMed: 21512573]

45. McWhirter SM, Fitzgerald KA, Rosains J, Rowe DC, Golenbock DT, and Maniatis T (2004). IFN-regulatory factor 3-dependent gene expression is defective in Tbk1-deficient mouse embryonic fibroblasts. Proceedings of the National Academy of Sciences of the United States of America 101, 233–238. 10.1073/pnas.2237236100. [PubMed: 14679297]

46. Song G, Liu B, Li Z, Wu H, Wang P, Zhao K, Jiang G, Zhang L, and Gao C (2016). E3 ubiquitin ligase RNF128 promotes innate antiviral immunity through K63-linked ubiquitination of TBK1. Nature immunology 17, 1342–1351. 10.1038/ni.3588. [PubMed: 27776110]

47. Tu D, Zhu Z, Zhou AY, Yun CH, Lee KE, Toms AV, Li Y, Dunn GP, Chan E, Thai T, et al. (2013). Structure and ubiquitination-dependent activation of TANK-binding kinase 1. Cell reports 3, 747–758. 10.1016/j.celrep.2013.01.033. [PubMed: 23453972]

48. Campbell EM, Weingart J, Sette P, Opp S, Sastri J, O'Connor SK, Talley S, Diaz-Griffero F, Hirsch V, and Bouamr F (2016). TRIM5alpha-Mediated Ubiquitin Chain Conjugation Is Required for Inhibition of HIV-1 Reverse Transcription and Capsid Destabilization. Journal of virology 90, 1849–1857. 10.1128/JVI.01948-15. [PubMed: 26676782]

49. Deng L, Wang C, Spencer E, Yang L, Braun A, You J, Slaughter C, Pickart C, and Chen ZJ (2000). Activation of the IkappaB kinase complex by TRAF6 requires a dimeric ubiquitin-conjugating enzyme complex and a unique polyubiquitin chain. Cell 103, 351–361. [PubMed: 11057907]

50. Fukushima T, Matsuzawa S, Kress CL, Bruey JM, Krajewska M, Lefebvre S, Zapata JM, Ronai Z, and Reed JC (2007). Ubiquitin-conjugating enzyme Ubc13 is a critical component of TNF receptor-associated factor (TRAF)-mediated inflammatory responses. Proceedings of the National Academy of Sciences of the United States of America 104, 6371–6376. 10.1073/pnas.0700548104. [PubMed: 17404240]

51. Garcia-Garcia J, Berge AKM, Overa KS, Larsen KB, Bhujabal Z, Brech A, Abudu YP, Lamark T, Johansen T, and Sjottem E (2023). TRIM27 is an autophagy substrate facilitating mitochondria

clustering and mitophagy via phosphorylated TBK1. The FEBS journal 290, 1096–1116. 10.1111/febs.16628. [PubMed: 36111389]

52. Wild P, Farhan H, McEwan DG, Wagner S, Rogov VV, Brady NR, Richter B, Korac J, Waidmann O, Choudhary C, et al. (2011). Phosphorylation of the autophagy receptor optineurin restricts Salmonella growth. Science 333, 228–233. 10.1126/science.1205405. [PubMed: 21617041]
53. Heo JM, Ordureau A, Swarup S, Paulo JA, Shen K, Sabatini DM, and Harper JW (2018). RAB7A phosphorylation by TBK1 promotes mitophagy via the PINK-PARKIN pathway. Science advances 4, eaav0443. 10.1126/sciadv.aav0443.
54. Sarraf SA, Raman M, Guarani-Pereira V, Sowa ME, Huttlin EL, Gygi SP, and Harper JW (2013). Landscape of the PARKIN-dependent ubiquitylome in response to mitochondrial depolarization. Nature 496, 372–376. 10.1038/nature12043. [PubMed: 23503661]
55. Li YL, Chandrasekaran V, Carter SD, Woodward CL, Christensen DE, Dryden KA, Pornillos O, Yeager M, Ganser-Pornillos BK, Jensen GJ, and Sundquist WI (2016). Primate TRIM5 proteins form hexagonal nets on HIV-1 capsids. eLife 5. ARTN e16269 10.7554/eLife.16269.
56. Di Rienzo M, Romagnoli A, Antonioli M, Piacentini M, and Fimia GM (2020). TRIM proteins in autophagy: selective sensors in cell damage and innate immune responses. Cell death and differentiation 27, 887–902. 10.1038/s41418-020-0495-2. [PubMed: 31969691]
57. Park SH, Han J, Jeong BC, Song JH, Jang SH, Jeong H, Kim BH, Ko YG, Park ZY, Lee KE, et al. (2023). Structure and activation of the RING E3 ubiquitin ligase TRIM72 on the membrane. Nature structural & molecular biology. 10.1038/s41594-023-01111-7.
58. Mirdita M, Schutze K, Moriwaki Y, Heo L, Ovchinnikov S, and Steinegger M (2022). ColabFold: making protein folding accessible to all. Nature methods 19, 679–682. 10.1038/s41592-022-01488-1. [PubMed: 35637307]
59. Yan Y, Tao H, He J, and Huang SY (2020). The HDOCK server for integrated protein-protein docking. Nat Protoc 15, 1829–1852. 10.1038/s41596-020-0312-x. [PubMed: 32269383]
60. Mandell MA, Jain A, Arko-Mensah J, Chauhan S, Kimura T, Dinkins C, Silvestri G, Munch J, Kirchhoff F, Simonsen A, et al. (2014). TRIM Proteins Regulate Autophagy and Can Target Autophagic Substrates by Direct Recognition. Developmental cell 30, 394–409. 10.1016/j.devcel.2014.06.013. [PubMed: 25127057]
61. Liu J, Lu S, Zheng L, Guo Q, Cao L, Xiao Y, Chen D, Zou Y, Liu X, Deng C, et al. (2023). ATM-CHK2-TRIM32 axis regulates ATG7 ubiquitination to initiate autophagy under oxidative stress. Cell reports 42, 113402. 10.1016/j.celrep.2023.113402. [PubMed: 37943659]
62. Narendra D, Tanaka A, Suen DF, and Youle RJ (2008). Parkin is recruited selectively to impaired mitochondria and promotes their autophagy. The Journal of cell biology 183, 795–803. 10.1083/jcb.200809125. [PubMed: 19029340]
63. Chan EY, Kir S, and Tooze SA (2007). siRNA screening of the kinome identifies ULK1 as a multidomain modulator of autophagy. The Journal of biological chemistry 282, 25464–25474. [PubMed: 17595159]
64. Chen X, and Prywes R (1999). Serum-induced expression of the cdc25A gene by relief of E2F-mediated repression. Molecular and cellular biology 19, 4695–4702. 10.1128/MCB.19.7.4695. [PubMed: 10373518]
65. Kamitani T, Kito K, Nguyen HP, and Yeh ET (1997). Characterization of NEDD8, a developmentally down-regulated ubiquitin-like protein. The Journal of biological chemistry 272, 28557–28562. 10.1074/jbc.272.45.28557. [PubMed: 9353319]
66. Lim KL, Chew KC, Tan JM, Wang C, Chung KK, Zhang Y, Tanaka Y, Smith W, Engelender S, Ross CA, et al. (2005). Parkin mediates nonclassical, proteasomal-independent ubiquitination of synphilin-1: implications for Lewy body formation. The Journal of neuroscience : the official journal of the Society for Neuroscience 25, 2002–2009. 10.1523/JNEUROSCI.4474-04.2005. [PubMed: 15728840]
67. Pankiv S, Clausen TH, Lamark T, Brech A, Bruun JA, Outzen H, Overvatn A, Bjorkoy G, and Johansen T (2007). p62/SQSTM1 binds directly to Atg8/LC3 to facilitate degradation of ubiquitinated protein aggregates by autophagy. The Journal of biological chemistry 282, 24131–24145. [PubMed: 17580304]

68. Jain A, Lamark T, Sjottem E, Larsen KB, Awuh JA, Overvatn A, McMahon M, Hayes JD, and Johansen T (2010). p62/SQSTM1 is a target gene for transcription factor NRF2 and creates a positive feedback loop by inducing antioxidant response element-driven gene transcription. The Journal of biological chemistry 285, 22576–22591. 10.1074/jbc.M110.118976. [PubMed: 20452972]

69. Bjorkoy G, Lamark T, Brech A, Outzen H, Perander M, Overvatn A, Stenmark H, and Johansen T (2005). p62/SQSTM1 forms protein aggregates degraded by autophagy and has a protective effect on huntingtin-induced cell death. The Journal of cell biology 171, 603–614. [PubMed: 16286508]

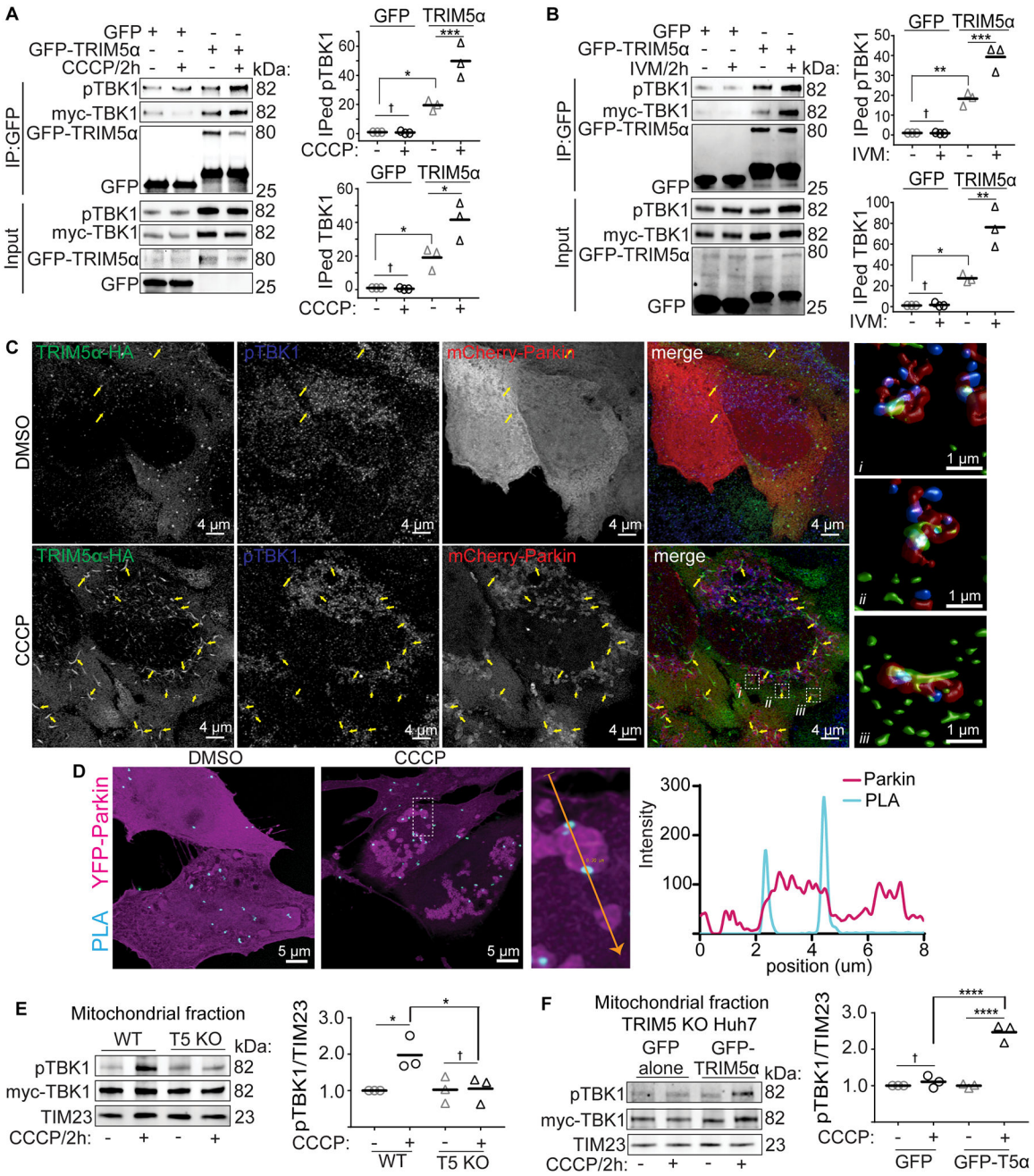

Figure 1. TRIM5α interacts with TBK1 and promotes its localization to damaged mitochondria.

(A, B) Coimmunoprecipitation analysis of TRIM5α/TBK1 interactions 2 hours after treatment with mitochondrial damaging agents CCCP (A) or invermectin (IVM) (B) or DMSO vehicle alone in transfected HEK293T cells. Plots show the relative abundance of immunoprecipitated (IPed) total TBK1 or phosphorylated TBK1 (pSer172) relative to the abundance of IPed GFP or GFP-TRIM5α. **(C)** Microscopic analysis of HeLa cells expressing TRIM5α-HA and mCherry-Parkin following 90 minutes treatment with CCCP or vehicle control (DMSO). Arrows indicate regions where TRIM5α and pTBK1 colocalize with each other and are contiguous to Parkin signal. Three-dimensional reconstructions of

the regions bounded by the dashed lines are shown to the right. **(D)** Proximity ligation assay (PLA, cyan) analysis of TRIM5α-HA interactions with pTBK1 in cells expressing YFP-Parkin (magenta) and treated or not with CCCP for 90 minutes. Intensity profile of the boxed region is shown at the right. **(E)** The abundance of total and pTBK1 in mitochondrial fractions from WT or TRIM5 knockout Huh7 cells treated or not with CCCP for 2 h. Plot shows the relative abundance of pTBK1 normalized to TIM23. Each data point represents an independent experiment. **(F)** Mitochondrial fractions were isolated from TRIM5 KO Huh7 cells expressing GFP-TRIM5α or GFP alone treated with DMSO or CCCP for 2 h. Quantitation of the relative abundance of pTBK1, normalized to TIM23, is shown at the right. Data: mean + SEM; *P* values determined by ANOVA with Tukey's multiple comparison test; *, $P < 0.05$; **, $P < 0.01$; ***, $P < 0.001$; ****, $P < 0.0001$; †, not significant.

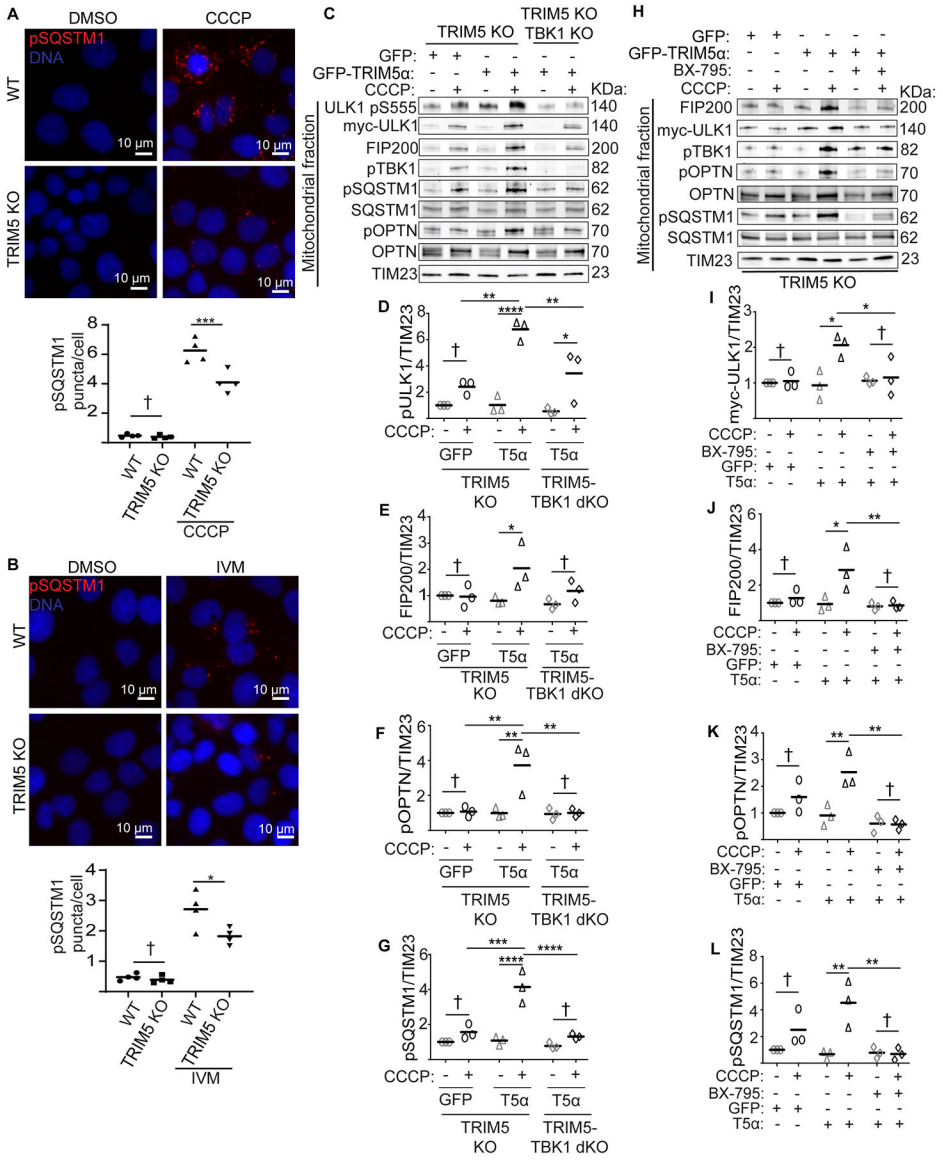

Figure 2. TRIM5α recruits autophagy machinery to damaged mitochondria in a TBK1-dependent manner.

(A, B) The number of phospho-SQSTM1 (pSer349) puncta was determined in WT and TRIM5 KO Huh7 cells following 2 h treatment with CCCP (A) or IVM (B) or DMSO alone by high content imaging. Each dot represents an individual experiment in which >500 cells were analyzed. **(C-G)** TRIM5 knockout or TRIM5/TBK1 double knockout (dKO) Huh7 cells were transfected with GFP-TRIM5α (T5α) or GFP alone as indicated and treated or not with CCCP (4 h) prior to isolation of mitochondrial fractions and immunoblotting (C). The abundance of the indicated proteins was determined, normalized to TIM23, and plotted (D-G). **(H-L)** TRIM5 KO Huh7 cells were transfected with GFP-TRIM5α (T5α) or GFP alone and treated or not with CCCP for 4 hours in the presence or absence of BX-795 prior to isolation of mitochondrial fractions and immunoblotting. The results of three independent experiments are quantitated in I-L. TIM23 was used as a loading control. Data: mean +

SEM; *P* values determined by ANOVA with Tukey's multiple comparison test; *, $P < 0.05$; **, $P < 0.01$; ***, $P < 0.001$; ****, $P < 0.0001$; †, not significant.

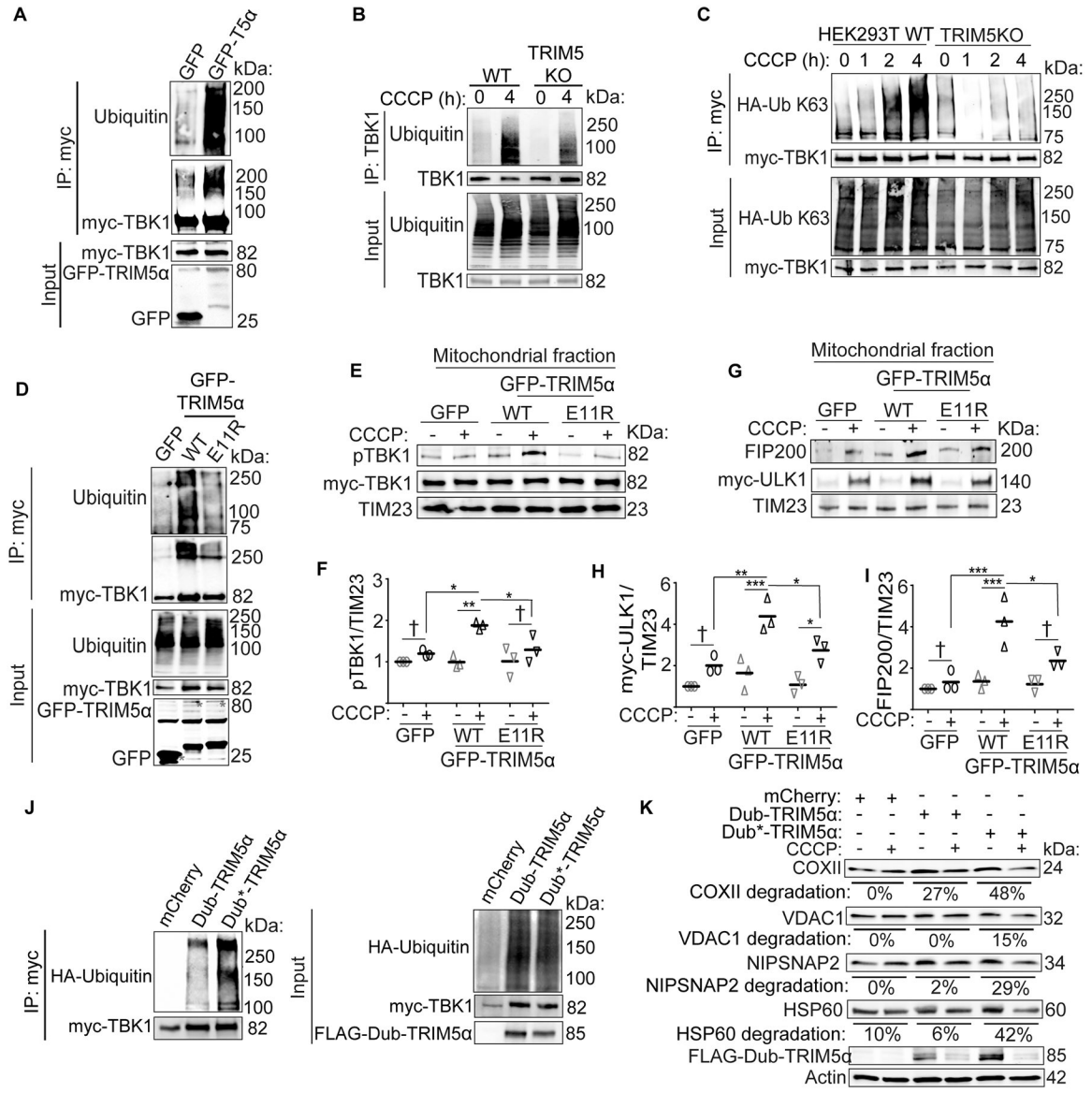

Figure 3. TRIM5α's ubiquitin ligase activity is required for K63-linked poly-ubiquitination of TBK1 and for mitophagy.

(A) Coimmunoprecipitation analysis of TBK1 ubiquitination in transfected HEK293T cells. **(B)** The effect of CCCP treatment on TBK1 ubiquitination in WT and TRIM5 knockout Huh7 cells. Endogenous TBK1 was immunoprecipitated and immunoblots were probed as indicated. **(C)** The effect of CCCP treatment on the K63-linked poly-ubiquitination of TBK1 in WT or TRIM5 KO HEK293T cells. **(D)** Coimmunoprecipitation analysis of TBK1 ubiquitination in HEK293T cells expressing GFP alone or GFP-tagged WT or E11R TRIM5α. Red * indicate GFP or GFP-TRIM5α bands of the expected molecular weight. **(E, F)** Mitochondrial fractions were obtained from TRIM5 knockout Huh7 cells transfected as indicated and treated or not with CCCP for 2 h. **(G-I)** The abundance of the indicated proteins in mitochondrial fractions isolated from TRIM5 knockout Huh7 cells transfected as shown and treated or not with CCCP. **(J)** Coimmunoprecipitation analysis of TBK1

ubiquitination in HEK293T cells transfected with myc-TBK1 and TRIM5α fused to either a catalytically active (Dub) or catalytically inactive (Dub*) deubiquitinase. mCherry was used as a negative control. **(K)** Relative degradation of mitochondrial proteins following CCCP treatment in TRIM5 knockout Huh7 cells transfected as indicated and treated or not with CCCP for 18 h. *P* values determined by ANOVA with Tukey's multiple comparison test; *, $P < 0.05$; **, $P < 0.01$; ***, $P < 0.001$; ****, $P < 0.0001$; †, not significant.

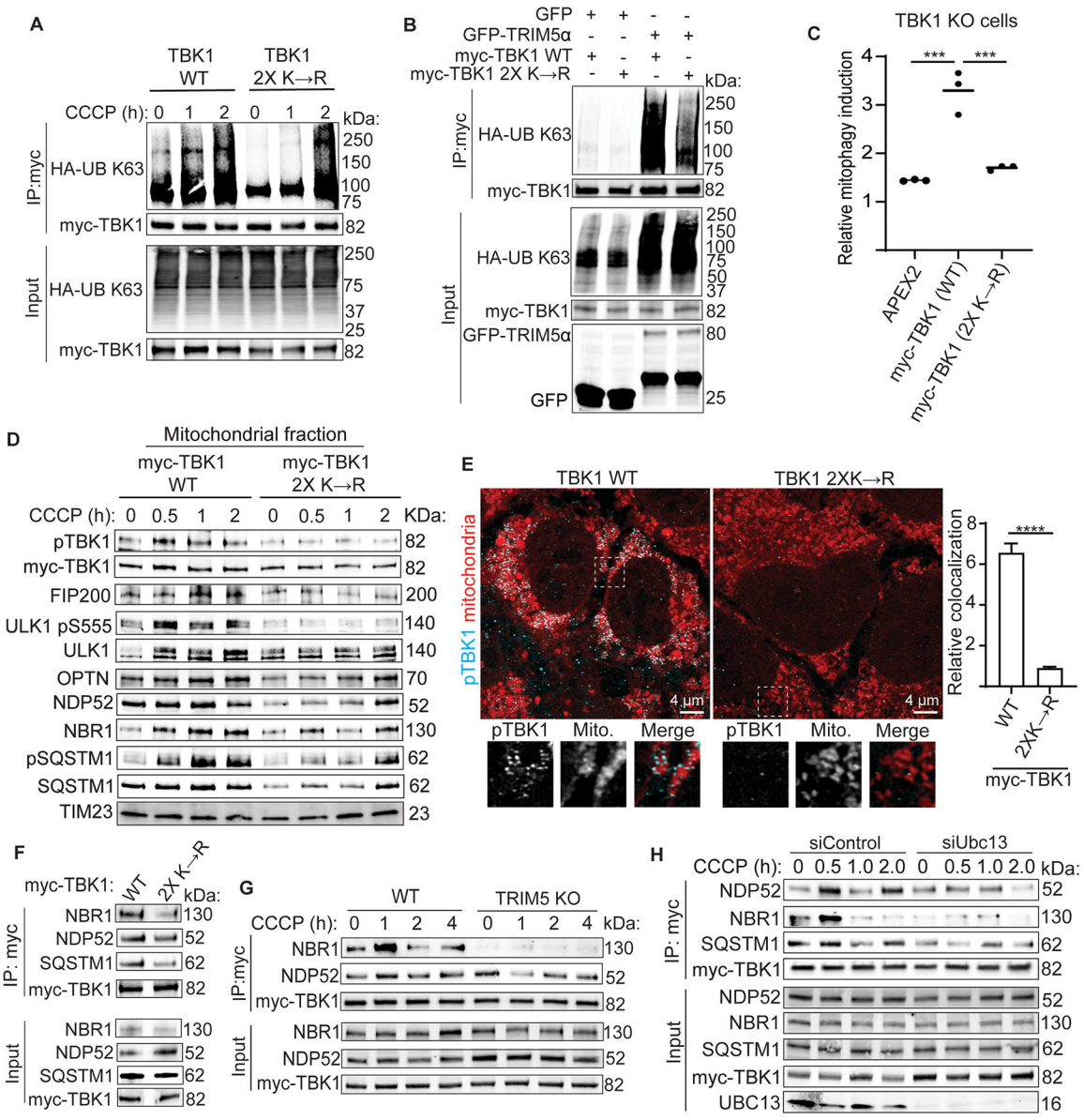

Figure 4. Ubiquitination of TBK1 at K30 and K401 by TRIM5α is required for mitophagy and enhances TBK1 interactions with autophagy adaptors.

(A) Coimmunoprecipitation analysis of TBK1 ubiquitination in transfected HEK293T cells and treated with CCCP for the indicated time points. **(B)** TBK1 ubiquitination assay in transfected HEK293T TRIM5KO cells. **(C)** TBK1 knockout cells expressing mito-mKeima were transfected with expression plasmids encoding WT or 2X K→R TBK1 or with an irrelevant control protein (APEX2) prior to a 6 h treatment with or without IVM and flow cytometry-based analysis of mito-mKeima fluorescence. Relative mitophagy induction is calculated by dividing the percentage of cells showing active mitophagy after IVM treatment by what is seen in DMSO alone-treated cells. See Figure S4A for flow cytometry data. **(D)** Immunoblot analysis of mitochondrial fractions isolated from transfected TBK1 knockout Huh7 cells following treatment with CCCP for the indicated time. **(E)** Left, colocalization of WT or 2X K→R mutant TBK1 with mitochondria in transfected TBK1 KO Huh7 cells

and treated with CCCP for 1 h. Zoomed-in images of the area within insets is shown below. Right, quantification of pTBK1 colocalization with mitochondria. The intensity of pTBK1 signal within voxels intersecting with mitochondria was normalized to the mitochondrial volume, multiplied by 10^7, and reported as "relative colocalization". N > 900 mitochondrial structures per treatment. *P* value determined by KS test**. (F)** Coimmunoprecipitation analysis of interactions between WT or 2X K→R TBK1 mutant and endogenous autophagy adaptors NBR1, NDP52, and SQSTM1 from transfected HEK293T cells. **(G)** The impact of TRIM5 knockout on CCCP-induced interactions between myc-TBK1 and endogenous NDP52 or NBR1. **(H)** CoIP analysis of interactions between TBK1 and autophagy adaptors in cells transfected with control or Ubc13 siRNA and treated for the indicated amount of time with CCCP. **, $P < 0.01$; ****, $P < 0.0001$.

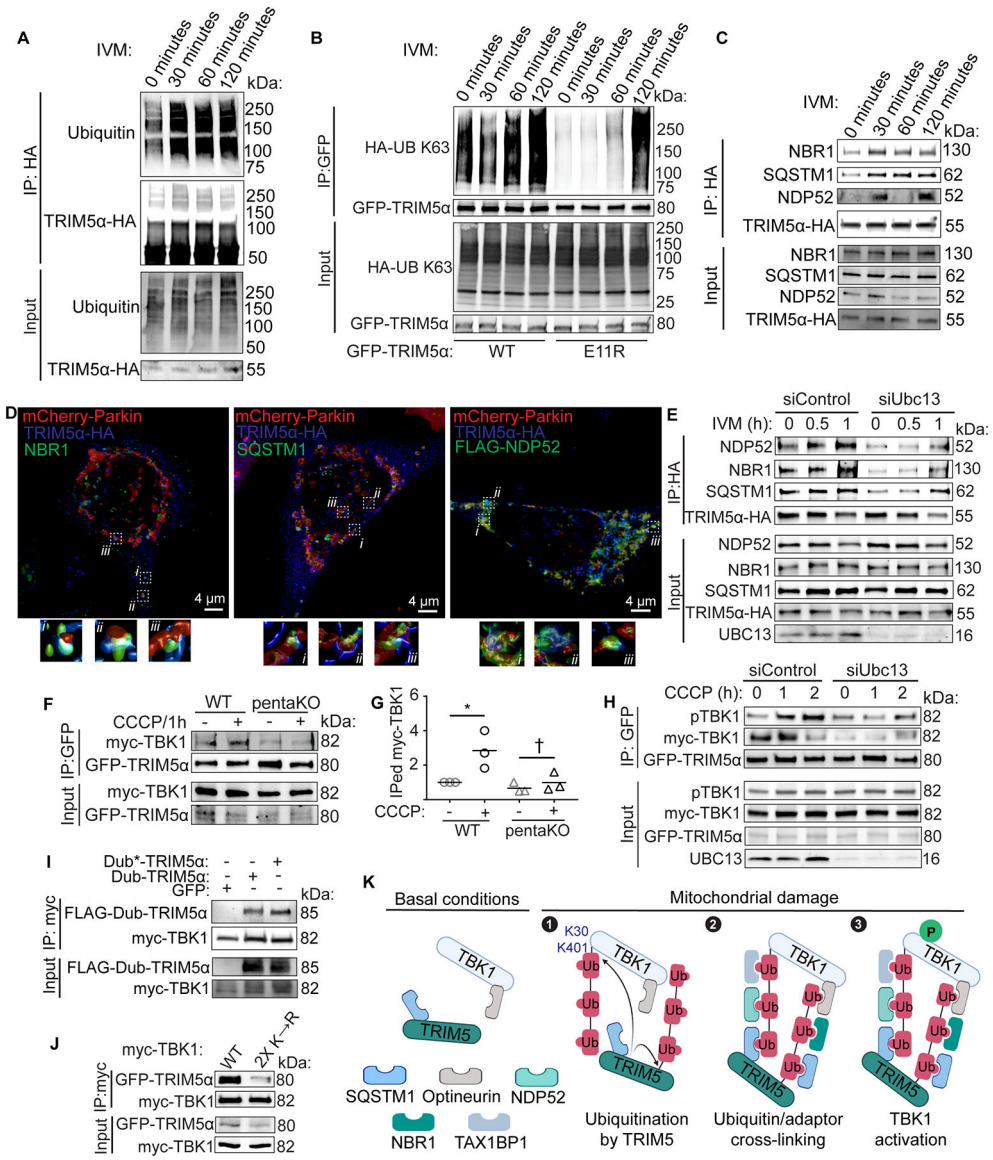

Figure 5. Interactions between TRIM5α and TBK1 are mediated by ubiquitin-binding autophagy receptors.

(A) Coimmunoprecipitation analysis of TRIM5α ubiquitination in HeLa cells treated with IVM for the indicated time points. **(B)** Analysis of K63-linked ubiquitination of WT or E11R TRIM5α following IVM treatment of transfected TRIM5α-knockout HEK293T cells. **(C)** Coimmunoprecipitation analysis of interactions between HA-TRIM5 and autophagy receptors from HeLa cell lysate following treatment with IVM. **(D)** Confocal microscopic analysis of the localization of TRIM5-HA, mCherry-Parkin, and autophagy adaptors in HeLa cells treated with CCCP for 90 minutes. 3D reconstructions of the boxed-in regions are shown below. **(E)** Coimmunoprecipitation analysis of TRIM5α interactions with autophagy adaptors following ivermectin treatment in cells transfected with control or Ubc13 siRNA. **(F, G)** Coimmunoprecipitation analysis of interactions between GFP-TRIM5α and myc-TBK1 in HeLa cells lacking all five autophagy adaptors (pentaKO) or parental HeLa cells treated or not with CCCP for 1 h. Both WT and pentaKO cells were also

transfected with mCherry-Parkin. The abundance of immunoprecipitated (IPed) myc-TBK1 was determined from three independent experiments, normalized to IPed GFP-TRIM5α, and plotted in (G). *P* values determined by ANOVA with Tukey's multiple comparison test; *, $P < 0.05$; †, not significant. **(H)** The impact of Ubc13 knockdown on interactions between GFP-TRIM5α and myc-TBK1 in HEK293T cells treated with CCCP for the indicated time as determined by co-immunoprecipitation with anti-GFP antibodies. **(I)** Lysates from HEK293T cells transfected with myc-TBK1 and TRIM5α fused to an active deubiquitinase (Dub) or a catalytically inactive deubiquitinase (Dub*) with an N-terminal FLAG tag were subjected to immunoprecipitation with anti-myc prior to immunoblotting as shown. GFP was used as a negative control. **(J)** Coimmunoprecipitation analysis of interaction between GFP-TRIM5α and WT or 2X K→R mutant myc-TBK1 in HEK293T TRIM5 KO cells. **(K)** Proposed mechanism for mitochondrial-damage induced TRIM5α-TBK1 interactions mediated by K63-linked ubiquitin chains.

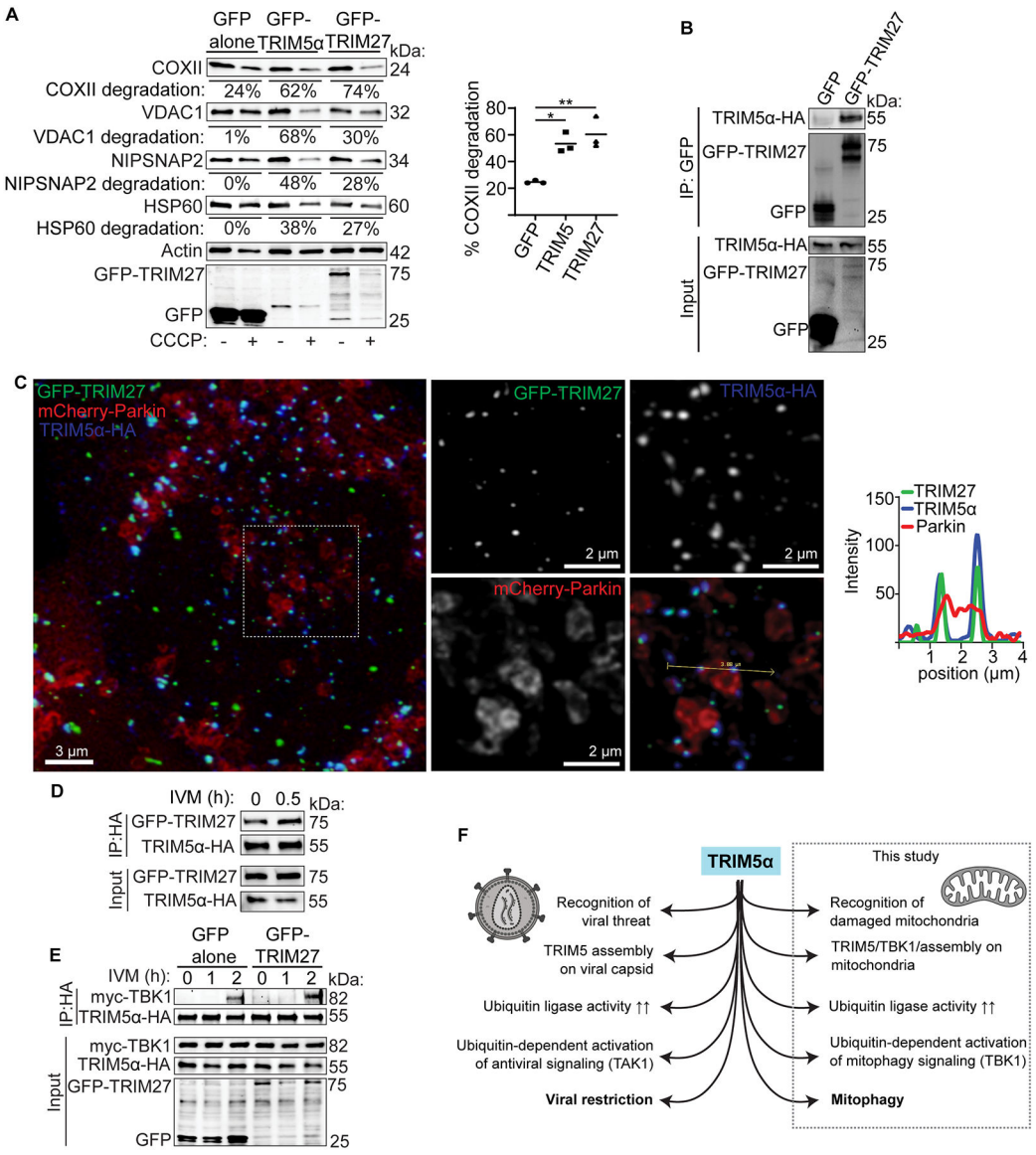

Figure 6. TRIM27 can restore mitophagy in cells lacking TRIM5α.

(A) Immunoblot analysis of mitochondrial protein abundance in TRIM5 knockout Huh7 cells transfected with GFP-TRIM5α, GFP-TRIM27, or GFP alone and treated or not with CCCP for 18 h. Plot shows the relative extent of COXII degradation following CCCP treatment for three independent experiments. **(B)** Coimmunoprecipitation analysis of interactions between GFP alone or GFP-TRIM27 and HA-TRIM5α in HeLa cells. **(C)** HeLa cells expressing TRIM5α-HA, GFP-TRIM27, and mCherry-Parkin were treated with CCCP for 90 m prior to fixation and confocal microscopy. The boxed in region (left) is shown on the right, along with an intensity profile showing colocalization between TRIMs on Parkin-labeled mitochondria. **(D)** Coimmunoprecipitation analysis of TRIM5α and TRIM27 interactions in HeLa cells treated with IVM for the indicated time points. **(E)** Lysates from HeLa cells expressing TRIM5α-HA, myc-TBK1, and either GFP-TRIM27 or GFP alone and treated with IVM for the indicated time were subjected to immunoprecipitation with

anti-HA and immunoblotted as indicated. **(F)** Comparison of TRIM5α actions in retroviral restriction with its actions in mitophagy. *P* values determined by ANOVA with Tukey's multiple comparison test; *, $P < 0.05$; **, $P < 0.01$.

Key resources table

REAGENT or RESOURCE	SOURCE	IDENTIFIER
Antibodies		
Phospho-TBK1/NAK (Ser172) (D52C2) Rabbit mAb	Cell Signaling Technology	*#5483, RRID: AB_10693472*
Phospho-ULK1 (Ser555) (D1H4) Rabbit mAb	Cell Signaling Technology	*#5869, RRID: AB_10707365*
TBK1/NAK (D1B4) Rabbit mAb	Cell Signaling Technology	*#3504, RRID: AB_2255663*
Phospho-SQSTM1/p62 (Ser349) Rabbit mAb	Cell Signaling Technology	*#95697, RRID: AB_2800251*
UBE2N (D2A1) Rabbit mAb	Cell Signaling Technology	*#6999, RRID: AB_10828936*
Atg13 (E1Y9V) Rabbit mAb	Cell Signaling Technology	*#13468, RRID: AB_2797419*
ULK1 (D8H5) Rabbit mAb	Cell Signaling Technology	*#8054, RRID: AB_11178668*
TRIM5 (D6Z8L) Rabbit mAb	Cell Signaling Technology	*#14326, RRID: AB_2798451*
Atg9A (D4O9D) Rabbit mAb	Cell Signaling Technology	*#13509, RRID: AB_2798241*
Anti-Tim23 Antibody (H-8)	Santa Cruz Biotechnology	**sc-514463**, RRID: AB_2923126
Anti-Optineurin Antibody (C-2)	Santa Cruz Biotechnology	**sc-166576**, RRID: AB_2156554
Anti-CALCOCO2 Antibody (F-6)	Santa Cruz Biotechnology	**sc-376540**, RRID: AB_11150487
Anti-NBR1 Antibody (4BR)	Santa Cruz Biotechnology	*sc-130380, RRID: AB_2149402*
Anti-Actin Antibody (2Q1055)	Santa Cruz Biotechnology	**sc-58673**, RRID: AB_2223345
Anti-GFP antibody	Abcam	ab290, **RRID: AB_303395**
Anti-HA tag antibody - ChIP Grade	Abcam	*ab9110, RRID: AB_2223345*
Anti-mCherry antibody	Abcam	*ab183628, RRID: AB_2650480*
Anti-MTCO2 antibody [12C4F12]	Abcam	*ab110258, RRID: AB_10887758*
MYC tag Polyclonal antibody	Proteintech	*16286-2-AP, RRID: AB_11182162*
RB1CC1 Polyclonal antibody	Proteintech	**17250-1-AP**, RRID: AB_10666428
Anti-Multi Ubiquitin mAb (Monoclonal Antibody)	MBL International	*D058-3, RRID: AB_592937*
Rabbit Anti-LC3B	Sigma Aldrich	*L7543, RRID: AB_796155*
Monoclonal ANTI-FLAG® M2 antibody produced in mouse	Sigma Aldrich	*L7543, RRID: AB_262044*
Purified Mouse Anti-p62 Ick ligand	BD biosciences	*P0067, RRID: AB_398151*
IRDye® 680LT Goat anti-Mouse IgG Secondary Antibody	LI-COR Biosciences	*925-68020, RRID: AB_2687826*
IRDye 800CW Goat anti-Mouse IgG, 0.1 mg	LI-COR Biosciences	*925-32210, RRID: AB_2687825*
Goat Anti-Mouse IgG (H+L)-HRP Conjugate	BIO-RAD	*1721011, RRID: AB_2617113*
Goat Anti-Rabbit IgG (H+L)-HRP Conjugate	BIO-RAD	*1721019, RRID: AB_11125143*
Mouse TrueBlot® ULTRA: Anti-Mouse Ig HRP, Rat Monoclonal eB144	Rockland	*18-8817-30, RRID: AB_2610849*
Clean-Blot™ IP Detection Reagent (HRP)	ThermoFisher	*21230, RRID: AB_2864363*
Goat anti-Mouse IgG (H+L) Highly Cross-Adsorbed Secondary Antibody, Alexa Fluor Plus 488	ThermoFisher	*A32723, RRID: AB_2633275*
Goat anti-Rabbit IgG (H+L) Highly Cross-Adsorbed Secondary Antibody, Alexa Fluor 488	ThermoFisher	*A-11034, RRID: AB_2576217*
Goat anti-Rabbit IgG (H+L) Cross-Adsorbed Secondary Antibody, Alexa Fluor 568	ThermoFisher	*A-11011, RRID: AB_143157*
Goat anti-Mouse IgG (H+L) Highly Cross-Adsorbed Secondary Antibody, Alexa Fluor Plus 647	ThermoFisher	*A32728, RRID: AB_2633277*

REAGENT or RESOURCE	SOURCE	IDENTIFIER
Goat anti-Rabbit IgG (H+L) Highly Cross-Adsorbed Secondary Antibody, Alexa Fluor Plus 647	ThermoFisher	*A32733, RRID: AB_2633282*
Bacterial and virus strains		
NEB 5-alpha Competent *E.coli* (High Efficiency)	New England Biolabs	C2987
XL10-Gold Ultracompetent cells	Agilent	210518
Chemicals, peptides, and recombinant protein		
Tetracycline hydrochloride	Sigma Aldrich	T3383
Puromycin dihydrochloride	Sigma Aldrich	P9620
BX-795 hydrochloride	Sigma Aldrich	SML0694
5Z-7-Oxozeaenol	Sigma Aldrich	O9890
Carbonyl cyanide 3-chlorophenylhydrazone (CCCP)	Sigma Aldrich	C2759
Ivermectin	Sigma Aldrich	I8898
2-mercaptoethanol	Sigma Aldrich	M3148
Phenylmethanesulfonyl fluoride solution	Sigma Aldrich	93482
cOmplete™, Mini, EDTA-free Protease Inhibitor Cocktail	Sigma Aldrich	11836170001
PHOSSTOP	Sigma Aldrich	4906837001
Saponin	Sigma Aldrich	84510
Tween 20	Sigma Aldrich	P1379
Leu-Leu methyl ester hydrobromide	Sigma Aldrich	L7393
1, 10- phenanthroline monohydrate	Sigma Aldrich	P9375
Dynabeads Protein G	ThermoFisher	10003D
IP lysis buffer	ThermoFisher	87788
RIPA lysis buffer	ThermoFisher	89901
Opti-MEM Reduced Serum Medium	ThermoFisher	31985070
Lipofectamine 2000 Reagent	ThermoFisher	11668019
Restore Plus Western Blot Stripping Buffer	ThermoFisher	46430
Hoechst 33342	ThermoFisher	H3570
10x Tris/Glycine/SDS buffer	Bio-Rad	1610732
2x Laemmli Buffer	Bio-Rad	1610737
4x Laemmli Buffer	Bio-Rad	1610747
Clarity ECL	Bio-Rad	1705061
Glycine	Bio-Rad	1610718
Tris Base	Bio-Rad	1610719
Sodium Chloride	VWR	BDH928625KG
Sodium Phosphate Dibasic	VWR	97061472
Potassium Chloride	VWR	EMPX14051
Potassium Phosphate Monobasic	VWR	EMDPX15651
Kanamycin Sulfate	VWR	97061-600
Ampicillin Sodium Salt	VWR	IC19014805
Dimethyl Sulfoxide(DMSO)	VWR	EMMX14586

REAGENT or RESOURCE	SOURCE	IDENTIFIER
Ethanol	VWR	89125172
Methanol	VWR	BDH20291GLP
2-Propanol (Isopropyl Alcohol)	VWR	BDH20271GLP
Triton X-100	VWR	EM9410
Paraformaldehyde	VWR	JTS8987
PR-619	UBPBio	F2110
PP242	LC Laboratories	P-6666
Blasticidin	Invivogen	Ant-bl-1
Hygromycin	Corning	30-240-CR
MG132	Selleckchem	S21619
PhenoVue™ 641 Mitochondrial Stain	PerkinElmer	CP3D1
Bovine Serum Albumin	Fisher Scientific	CAS 9048-46-8
Critical commercial assays		
ProFection Mammalian Transfection System	Promega	E1200
Dual-Glo Luciferase	Promega	E2920
QProteome mitochondria isolation kit	Qiagen	37612
Duolink® In Situ PLA® Probe Anti-Rabbit PLUS	Sigma Aldrich	DUO92002
Agilent QuikChange Lightning Site-Directed Mutagenesis Kit	Agilent	210518
Experimental models: Cell lines		
HEK293T TRIM5 knockout	Saha et al, 2022[31]	N/A
HeLa TRIM5 knockout	Saha et al, 2022[31]	N/A
HeLa HumanTRIM5α-HA	Stremlau et al, 2004[33]	N/A
HeLa cells stably expressing YFP-Parkin	Narendra et al, 2008[62]	N/A
Huh7 TRIM5 knockout	Saha et al, 2022[31]	N/A
Huh7 WT cells stably expressing mt-mkeima	This study	N/A
Huh7 TRIM5 knockout cells stably expressing mt-mkeima	This study	N/A
Huh7 TBK1 knockout cells stably expressing mt-mkeima	This study	N/A
Huh7 TRIM5-TBK1 DKo	This study	N/A
HEK293T TBK1 knockout	This study	N/A
HeLa WT and Penta KO	Lazarou et al, 2015[9]	N/A
Oligonucleotides		
Primers for GFP-TRIM5 L19R Sense: Fw, CTGCCCCATCTGCCGGGAACTCCTGACAC Antisense: Rw, GTGTCAGGAGTTCCCGGCAGATGGGGCAG	Integrated DNA Technologies	N/A
Primers for TBK1 K30R Sense: Fw, GATAGCAAATAAATCACCAGTTCTCTTATGTCTTCCACGAAAGACA Antisense: Rw, TGTCTTTCGTGGAAGACATAAGAGAACTGGTGATTTATTTGCTATC Primers for TBK1 K401R Sense: Fw, CTAAATCATAACGTGGATGTACTCTAGGGAGGGAAATTTTTTCAT	Integrated DNA Technologies	N/A

REAGENT or RESOURCE	SOURCE	IDENTIFIER
ATATT Antisense: Rw, AATATATGAAAAAATTTCCCTCCCTAGAGTACATCCACGTTATGAT TTAG		
Recombinant DNA		
GFP-TRIM5α	Stremlau et al 2004[33]	N/A
myc-TBK1	Pilli et al 2012[28]	N/A
YFP-Parkin	Narendra et al., 2008[62]	Addgene, 23955
mCherry-Parkin	Narendra et al., 2008[62]	Addgene, 23956
mito-mkeima	Vector builder	Ecoli(VB231119-1373wjt)
myc-ULK1	Chan et al 2007[63]	N/A
NF-κB luciferase plasmid	Promega	E8491
pRL-SV40P	Chen et al., 1999[64]	Addgene, 27163
pGL4.33[*luc2P*/SRE/Hygro]	Promega	E8491
psPAX2	Trono et al.,	Addgene,12260
pMD2.G	Trono et al.,	Addgene,12259
HA-ubiquitin	Kamitani et al., 1999[65]	Addgene,18712
HA-ubiquitin K63	Lim et al., 2005[66]	Addgene,17606
GFP-TRIM5α E11R	Saha et al, 2022[31]	N/A
mCherry	Pankiv et al, 2007[67]	N/A
Dub-TRIM5α	Cambell et al, 2016[48]	N/A
Dub*-TRIM5α	Cambell et al, 2016[48]	N/A
GFP-TRIM5α L19R	This study	N/A
myc-TBK1 2X K→R	This study	N/A
FLAG-NDP52	Jain et al, 2010[68]	N/A
FLAG-OPTN	Jain et al, 2010[68]	N/A
FLAG-TAX1BP1	Jain et al, 2010[68]	N/A
FLAG-NBR1	Jain et al, 2010[68]	N/A
FLAG-SQSTM1	Jain et al, 2010[68]	N/A
GFP-TRIM5α RING deleted	Mandell et al, 2014[60]	N/A
GFP-TRIM5α B box deleted	Mandell et al, 2014[60]	N/A
GFP-TRIM5α CCD deleted	Mandell et al, 2014[60]	N/A
GFP-TRIM5α SPRY deleted	Mandell et al, 2014[60]	N/A
GST-NAP1	This study	N/A
GST-TRIM5α WT	This study	N/A
GST-TRIM5α 1-282	This study	N/A
GST	Bjorkoy et al, 2005[69]	N/A
GST-mAtg8s	Bjorkoy et al, 2005[69]	N/A
Software and algorithms		

REAGENT or RESOURCE	SOURCE	IDENTIFIER
Prism 8	GraphPad	N/A
Image Lab	BIO-RAD	N/A
FlowJo (v10.10.0)	BD Biosciences	N/A
iDEV software	ThermoFisher	N/A
Huygens Object Analyzer and Colocalization	Scientific Volume Imaging	N/A
LASX acquisition software	Leica	N/A
BioRender	BioRender.com	N/A